SYNTHESIS AND CHARACTERIZATION OF CYANURIC-BASED DYE-SENSITIZER FOR SOLAR CELLS, THEIR PHOTO-RESPONSE IN THE VISIBLE REGION AND CHEMOSENSING PROPERTIES

A MINI THESIS SUBMITTED IN PARTIAL FULFILMENT

OF THE REQUIREMENTS FOR THE DEGREE OF

MASTER OF SCIENCE IN CHEMISTRY

OF

THE UNIVERSITY OF NAMIBIA

BY

MABUKU SIMASIKU DAN

201202873

APRIL 2021

SUPERVISOR: PROF. V. UAHENGO (UNIVERSITY OF NAMIBIA)

ABSTRACT

Two cyanuric-based potential dye-sensitizers were synthesized (**Dye 1** & **Dye 2**), and characterized spectroscopically, UV-vis and FTIR among other techniques. Their photoresponse properties in the visible region were investigated (in ethanol at 1×10^{-5}M) and studied. In addition, solvatochromic effect was also investigated, in solvents such as acetonitrile, ethyl acetate, ethanol, methanol and toluene. It was established that both dyes have good solubility in ethanol and acetonitrile, compared to the others. Photophysical measurements suggest that the compounds display fitting light absorption characteristics for use as sensitizer in dye-sensitized solar cells (DSSCs), with absorption maxima centered in the visible region in both cases. However, **Dye 2** (compared to **Dye 1**) is highly likely to be more functional as a solar material, as evidenced by its wide absorption range in the visible region resulting from its appropriate charge transfer mechanism, the intramolecular charge transfer (ICT), which may translate into enhanced photon harvesting. In addition, **Dye 1** & **Dye 2** can function as chemosensors by exploiting the same ICT mechanism, which makes them suitable for dye sensitizers. Subsequently, upon conducting UV-Vis analysis, **Dye 1** appears to have selective recognition of Al^{3+} and Cu^{2+}, whereas **Dye 2** has a selective recognition of Pb^{2+} from all the cations that they were tested against (Al^{+}, Co^{2+}, Cr^{2+}, Cu^{2+}, Fe^{2+}, K^{+}, Li^{+}, Pb^{2+}). Similarly, **Dye 1** and **Dye 2** were also tested against anions (SO_4^{2-}, AcO^{-}, Br^{-}, CN^{-}, F^{-}, NO_3^{-} and PO_4^{3-}), in which **Dye 1** demonstrated selective recognition of SO_4^{2-}, CN^{-}, PO_4^{2-} and F^{-} , while **Dye 2** has selective recognition of ONLY SO_4^{2-} and F^{-}. Thus, **Dye 1** & **Dye 2** are both classified as dual sensors, for possessing more than one recognition site with its structural framework.

Table of Contents

ABSTRACT i
LIST OF SCHEMES v
LIST OF FIGURES vi
LIST OF ABBREVIATIONS AND/OR ACRONYMS viii
ACKNOWLEDGEMENTS ix
DEDICATION x
DECLARATIONS xi
1. INTRODUCTION 1
1.1 Background of the study 1
1.2 Statement of the problem 1
1.3 Objectives of the study 3
1.4 Significance of the study 3
1.5 Limitation of the study 3
1.6 Delimitation of the study 3
2. LITERATURE REVIEW 4
2.1 Background 4
2.2 Working principle 5
2.3 The notion of sensitisation 6
2.4 Structure 8
2.5 Absorption spectrometry 9
3. RESEARCH METHODS 11
3.1 Research Design 11
3.2 Procedure 11
3.2.1 Synthesizing the dyes 11
3.2.2 Investigating the effect of solvatochromism 12
3.2.3 Characterizing the organic-based DSSCs using spectroscopic techniques 12
3.2.4 Investigating their photo-response in the visible region 12
3.2.5 Investigating the chemosensing properties 12
3.3 Data Analysis 12
4. EXPERIMENT 13
4.1 Materials and Instruments 13
4.2 Synthesis of the dyes 13
5. RESULTS AND DISCUSSIONS 16

5.1. Photophysical property studies of the dyes 16
5.2 Solvatochromic studies of the dyes 17
5.2.1 Solvatochromic effect on optoelectronic properties of the dyes 20
5.3 Infrared analysis of the dyes 20
5.4 Naked eye detection test 22
5.4.1 Cation test 22
5.4.2 Anion test 23
5.5 UV–Vis binding interaction studies 25
5.5.1 UV-Vis for cation studies 25
5.5.2 UV-Vis for anion studies 27
6. CONCLUSIONS 32
7. RECOMENDATIONS 32
8 REFERENCES 33
APPENDICES 37

LIST OF TABLES

Table 1**:** UV-visible absorption maxima of **Dye 1** in different solvents; (Acetonitrile, Ethyl Acetate, Ethanol, Methanol and Toluene)..... 19

Table 2**:** UV-visible absorption maxima of **Dye 2** in different solvents; (Acetonitrile, Ethyl Acetate, Ethanol, Methanol and Toluene)..... 19

LIST OF SCHEMES

Scheme 1. Two cyanuric-bridged porphyrin dyads [13]…….9

Scheme 2. Synthesis of (a) Dye 1 and (b) Dye 2……...15

LIST OF FIGURES

Figure 1. Energy flow in the dye – sensitized solar cell [2]. 6

Figure 2. Dye-sensitizer solar cell system [19]. 7

Figure 3. UV–vis absorption spectra of a cyanuric-based dye (ZnP-triazine-$(gly)_2$) in THF solution (black color) and ZnP-triazine-$(gly)_2$ adsorbed onto TiO_2 film (red color) [23]. 10

Figure 4. Molecular structure of the target dyes 11

Figure 5. UV–Vis absorption spectra of Dye 1 in 1×10^{-5} mol·dm^{-3} Ethanol. 16

Figure 6. UV–Vis absorption spectra of Dye 2 in 1×10^{-5} mol·dm^{-3} Ethanol. 17

Figure 7. UV–Vis absorption spectra of (a) Dye 1 in 1×10^{-5}mol·dm^{-3} Acetonitrile, Ethyl Acetate, Ethanol, Methanol and Toluene; and (b) Dye 2 in 1×10^{-5}mol·dm^{-3} Acetonitrile, Ethyl Acetate, Ethanol, Methanol and Toluene. 18

Figure 8. Infrared (IR) spectra of (a) Dye 1 and (b) Dye 2. 22

Figure 9. Showing color changes of (a) Dye 1 and (b) Dye 2 in ethanol at 1×10^{-5}M, after the additions of the cations respectively. 23

Figure 10. Showing color changes of (a) Dye 1 and (b) Dye 2 in ethanol at 1×10^{-5}M, after the additions of the anions respectively. 24

Figure 11. UV–Vis spectra of Dye1 in 1×10^{-5}mol·dm^{-3} ethanol after the addition of (a) Al^{+} and (b) Cu^{2+} cations. 26

Figure 12. UV–Vis spectra of Dye 2 in 1×10^{-5}mol·dm^{-3} ethanol after the addition of Pb^{2+} cation. 27

Figure 13. UV–Vis spectra of Dye 1 in 1×10^{-5}mol·dm^{-3} ethanol after the addition of (a) CN^{-}, (b) SO_4^{2-}, (c) F^{-} and (d) PO_4^{3-} anions. 30

Figure 14. UV–Vis spectra of Dye 2 in 1×10^{-5}mol·dm^{-3} ethanol after the addition of (a) F^{-} and (b) SO_4^{2-} anions. 31

Figure 15. UV–Vis spectra of Dye 1 in 1 × 10^{-5}mol·dm^{-3} ethanol after the addition of (a) Br^-, (b) NO^-, (c) Co^{2+}, (d) Cr^{2+}, (e) Fe^{2+}, (f) K^+, (g) Li^+, (h) $Pb^{2+}$and (i) Zn^{2+}. 41

Figure 16. UV–Vis spectra of Dye 2 in 1 × 10^{-5}mol·dm^{-3} ethanol after the addition of (a) Br^-, (b) CN^-, (c) F^-, (d) NO^-, (e) PO_4^{3-}, (f) Fe^{2+}, (g) Al^+, (h) Co^{2+}, (i) Cr^{2+}, (j) Cu^{2+}, (k) L^+, (l) Zn^{2+}..... 47

Figure 17. Absorption spectrum of Dye 1 in different solvents and optical onset band gap respectively..... 48

Figure 18. Absorption spectrum of Dye 2 in different solvents and optical onset band gap respectively..... 48

LIST OF ABBREVIATIONS AND/OR ACRONYMS

DC – Direct Current

DSSC – Dye-Sensitized Solar Cell

e^- - Electron

p-n (in p-n junction) – Positive side-Negative side (frontier between two semiconductor material) [7]

Redox – Reduction-oxidation

THF – Tetrahydrofuran

UV-vis – Ultraviolet-visible

ACKNOWLEDGEMENTS

Firstly, acknowledgements go to the almighty God for great health to carry out the research. This work was supported by the University of Namibia, providing an environment to complete the research, the chemistry and biochemistry department staff together with Prof. V. Uahengo (supervisor) for constantly being supportive throughout. Furthermore, gratitude is extended to the Namibia University of Science and Technology for assistance in some analysis of samples.

DEDICATION

This thesis work is dedicated to my sons, Neddy L. Mabuku & Dan S. Mabuku, their mother Manyando L Ntabi and my mother Albertina M Sibeya who have loved me unconditionally and been a constant source of support and encouragement during the challenges of graduate school and life. I am truthfully blessed for having you in my life. This work is also dedicated to my Dog “Street”, he will not read this but he is one of the things dear to my heart. I dedicate this work to the gospel and give special thanks to God who made everything possible.

DECLARATIONS

I, **Dan Mabuku**, hereby declare that this study is my own work and is a true reflection of my research, and that this work, or any part thereof has not been submitted for a degree at any other institution.

……. …… ……

Name of Student **Signature** **Date**

1. INTRODUCTION

1.1 Background of the study

Through the past 20 years, dye-sensitized solar cells (DSSCs) have enticed substantial interest as low-cost alternatives to conventional photovoltaic technologies [1]. A dye-sensitized solar cell (DSSC) is a type of solar cell that employs the use of a dye to absorb sun rays on solar cells [2]. Over the years, quite a number of dyes have been tried as sensitizers, Among them, metal-free organic sensitizers have been advanced and studied extensively for their benefits of high extinction coefficients, varied design, hypothetically lower cost than metal complexes, stress-free preparation and purification [1]. Dye sensitizers are a very important component in dye sensitizer solar cells as they help with light harvesting and power conversion efficiency [3]. The structure of 1,3,5-triazine (Cyanuric) facilitates the synthesis of p-conjugated multi-chromophores dyes resulting in enhanced electron injection and transportation rates [4]. In addition, the same charge transfer mechanisms accounts for the sensitization process, are normally suitable for the discrimination of ionic species in different solvent mediums [5], through the process of chemosensing.

1.2 Statement of the problem

Energy demands are increasing due to technological advancement and population increase. The earth receives a lot of solar energy, as such scientists and researchers are coming up with new ways to utilize solar energy [6]. The supply-demand of energy is one of the most common problems to humans, considering the use of non-renewable resources of energy that is being used to satisfy human needs, however the continued use of non-renewable resources leads to their depletion, thus the need to satisfy the

energy earth's energy needs on a global scale using energy that can last a considerable amount of time. One favorable contender is solar energy, which is renewable, unpolluting, and an unlimited resource [7]. One way of converting solar energy to electrical energy is by using solar cells, however conventional solar cells are expensive to create, thus the rising interest in dye-sensitized solar cells (DSSCs) which are cheap and easy to construct. Capturing sunlight (solar energy) and converting it to useful electrical energy at a cost-effective level is still a challenge [8]. DSSCs have captivated significant attention due to their great solar energy-to-conversion efficiencies and low cost processes compared to conventional p–n junction solar cells [7]. In the past years, Zn(II) porphyrin complexes and Ru(II)-based chromophores have attained high efficiency, and as favorable sensitizers widely applied in DSSC field. However, in respect to the cost-effectiveness, environmentally pleasant, and low synthetic yield, these aspects could confine the possibly large-scale application of these complexes. Consequently, the plenty metal-free organic dyes that are abundant have appealed many attentions, they display countless advantages, such as higher molar extinction coefficient, lower cost and more facile in molecular design [9]. Because of these qualities, organic dyes have become popular in the DSSC field [9].

Cyanuric-based organic dyes make up a very significant class of compounds since they display potential as sensitizers for dye sensitized solar cells (DSSCs) and as donor materials for small molecule organic solar cells [10]. Thus organic-based dyes, cyanuric-based dyes in particular are synthesized to meet societal energy demands, plus as they are easy and inexpensive to synthesize, meaning they can be synthesized by almost anyone. They currently have a conversion efficiency just above 10%, and can get even better [4].

1.3 Objectives of the study

The objectives of the study were:

a. To synthesize cyanuric-based dye-sensitizer for solar cells
b. To investigate the effect of solvatochromism of the dyes
c. To investigate the dyes photo-response
d. To investigate the chemosensing properties of the synthesized dyes

1.4 Significance of the study

The research was aimed at synthesizing cyanuric-based DSSCs and also investigating how to enhance light harvesting in the DSSCs. Metal-free sensitizers currently have a conversion efficiency above 10% [11]. A lot of improvement can still be done to get the efficiency even higher to meet energy demands. Thus given the high potential of metal-free sensitizers, there is still a high possibility of improving their efficiency.

1.5 Limitation of the study

Some samples needed to be sent off-campus for analysis (^{1}H NMR) thus slowing down the progression of the research.

1.6 Delimitation of the study

This research was focusing on the characterization of the dyes to be synthesized and their chemosensing properties. Other applications such as assembling of DSSC were not be done.

2. LITERATURE REVIEW

2.1 Background

The exhaustion of limited fossil fuels together with the cumulative global demand for energy have indorsed the quest for clean, renewable, and cheap energy [12]. On the other hand, solar energy is being conveyed to the earth regularly. In particular, Namibia is a country that receives a considerable amount of sunlight. Solar energy is sustainable, renewable and environmental friendly. Accordingly, dye-sensitized solar cells are being advanced extensively to capture solar energy and convert it to usable electrical energy to encounter the global energy demand [12]. In 1991, O'Regan and Grätzel conveyed the first efficient DSSC [13]. The crucial features of a DSSC rely essentially on two modules; a dye and a wide band-gap semiconductor [14]. Organic dyes function as sensitizers, emitters, or charge transporters [15]. Thus, the synthesis and characterization of organic dyes retaining the above cited functional properties are aggressively pursued. Metal-free dyes have ample raw materials, are easy to synthesis and low cost to synthesize [16]. Cyanuric dyes containing conjugated aromatic cycles typically have decent light gathering capabilities [16]. Cyanuric dyes consist of an electron donor and an electron acceptor at two ends denoted as D-π-A, where D is electron donor and A is electron acceptor connected by a π-bridge [17]. The D-π-A structure makes an effective intramolecular charge transfer during photoexcitation [17]. Cyanuric-based sensitized solar cells show promising applications in many areas, such as chemosensors, and catalysis, they can be used as sensors to detect ions present in solution [5].

To increase the electrical current, there must be huge number of minority charge carriers, which cross the depletion region [6]. D-π-A type organic dyes show great spectral properties, but they usually aggregates on the semiconductor surface, however

the aggregates can be reduced by adding bulky substituents to the structure of the dye [17]. It is generally known that the DSSCs absorb light in the wavelength range between 400 and 700 nm and organic dyes in particular usually have an efficiency of around 11% [17]. Research on solar cells is being focused to try and broaden the range gap and to increase the efficiency of the DSSCs. Photons below a threshold wavelength about 920 nm should be harvested and converted into electric current [18].

2.2 Working principle

Titanium dioxide (TiO_2) is not sensitive to visible light. Thus the TiO_2 particles need to be sensitized with a coating of dye molecules that absorbs light in the visible region of the spectrum. It works in such a way that photon(s) derived from sun rays are absorbed by the dye, the dye gets excited and electrons are generated. Electrons move swiftly to the semiconductor, and then passed to the counter electrode, after which the electrons will move through the electrolyte solution (redox processes), and back again to the dye. Proses spin cycle continue to form, so that electrical current can be generated, this is shown in figure 1.

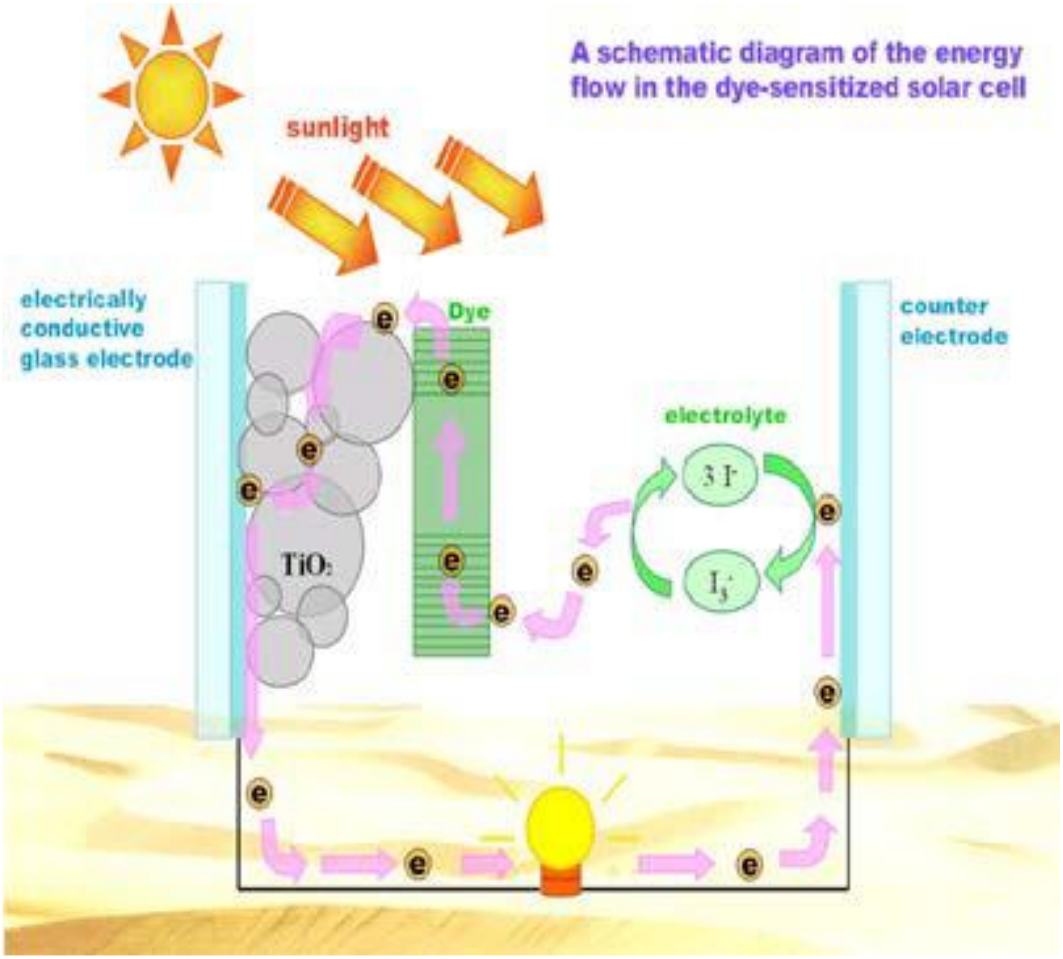

Figure 1. Energy flow in the dye – sensitized solar cell [2].

2.3 The notion of sensitisation

A dye-sensitized solar cell functions because of the interactions between the anode and cathode of the cell, and TiO_2 nanoparticles that are coated with a dye that is light-sensitive and surrounded by an electrolyte. The anode is transparent, like glass, such that sun rays can penetrate and be absorbed by the internal parts of the solar cell. TiO_2 nanoparticles are between the anode and cathode. The TiO_2 act like a highway for the electrons (electricity) flowing through the cell. The TiO_2 nanoparticles are coated with a dye that absorbs light (photons) and converts it to electricity. In a DSSC, the electrons flow from the cathode to the anode. The electrons (electricity) move through the electrolyte (I^-) and the TiO_2 nanoparticles to create an electric current. TiO_2

nanoparticles are transparent and generally used as conductors because of their exceptional capability to be ‘welded’ together and form one colossal network for the electrons to move through.

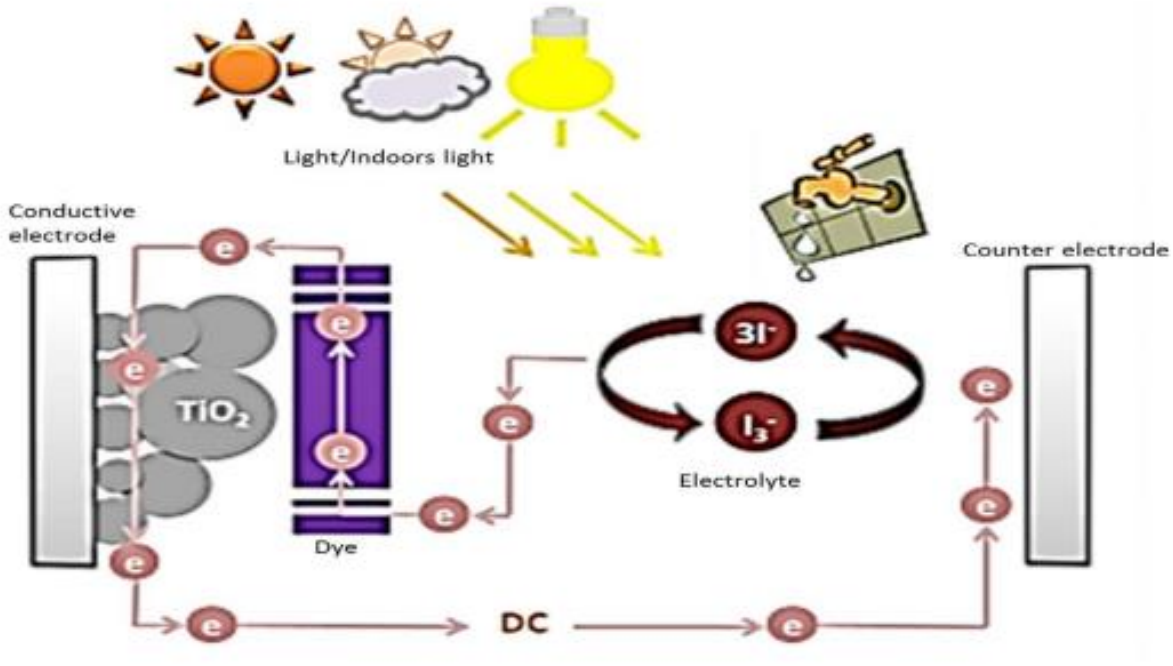

Figure 2. Dye-sensitizer solar cell system [19].

The electrons initiate from the dye coating the TiO_2 nanoparticles when they are hit by light (photons). Dyes of different colours absorb different wavelengths of light, as a result carry different quantities of energy. When the dye molecule absorb light photons, it enters an excited state and releases an electron. The released electron moves through the TiO_2 nanoparticles and reaches the anode, or is lost to I^- due to defects in the TiO_2 nanoparticles. The dye molecule will begin to decompose except it obtains an electron to substitute the one it lost. In this state, the dye molecule cannot emit any additional electrons. It is the reason the dye-coated TiO_2 molecules are engrossed in I^- solution because I^- ion is capable of replacing the electrons lost by the dye molecules. When this transpires, I^- ion oxidizes to I_3^-, which will float around until it comes in

contact with the cathode. Each I_3^- ion receives two electrons from the cathode, which reduces it back to three I^- ions [19].

2.4 Structure

The prodigious trend in designing organic dyes (cyanuric-based dyes) is based on a donor-π bridge-acceptor (D-π-A) architecture [1]. Dhirendra Kumar *et al*. [20] stated that the characteristic electron-rich moieties act as donors, furthermore, the π-spacer between the electron donor and electron acceptor tunes the absorption capability and photovoltaic performance. According to Chuan-Pei Lee *et al.* [21] in light illumination, the electrons convey through an intramolecular path in an organic dye: electron donor moiety - π-conjugated bridge/spacer - electron acceptor moiety - anchoring acid ligand, and then enter the TiO_2 network; this charge transfer occurrence is largely called the 'electron injection,' which is the core of solar-to-electricity conversion processes in a DSSC. A π-conjugated group that has been recently employed as a linker in the synthesis of metal-free organic dyes for DSSCs is 1,3,5-triazine (cyanuric) [13]. Galateia E. Zervaki *et al*. [13] state that the properties (structural, chemical and electronic) of this unit permit the synthesis of complex π-conjugated multi-chromophoric dyes through modest organic reactions that proffer enhanced light harvesting capability, as well as enhanced electron injection and transportation rates. Zervaki *et al*. [13] further reported two new triazine-bridged porphyrin dyads, 5a and 5b, the earlier with two carboxylic acid anchoring groups for connection to the TiO_2 surface, and the latter with one carboxylic acid anchoring group and a piperidine binding site, that has the prospective to perform as a supplementary anchoring group (Scheme 1).

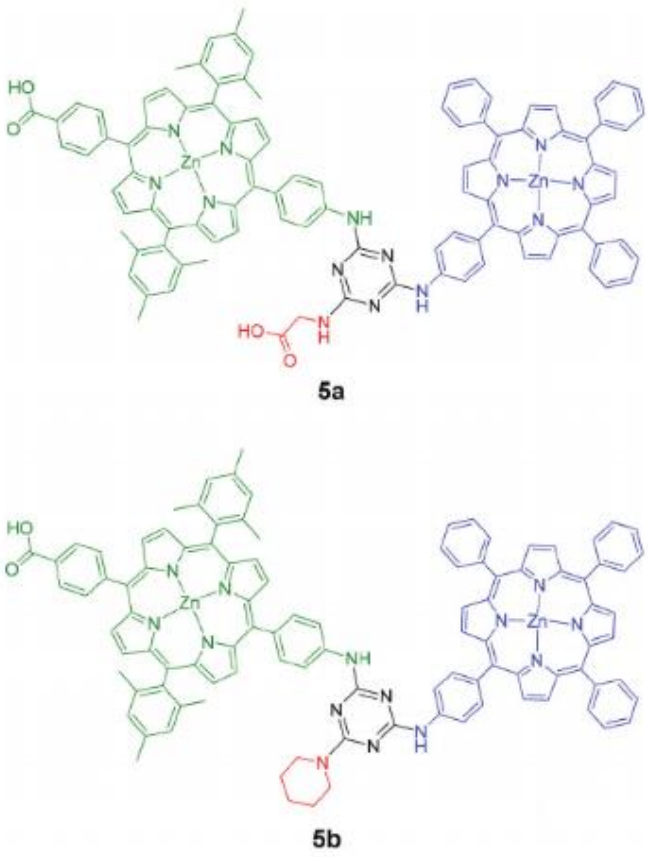

Scheme 1. Two cyanuric-bridged porphyrin dyads [13].

2.5 Absorption spectrometry

The UV absorption spectrum of cyanuric in cyclohexane shows two bands at 272 nm and 222 nm due to the $\pi \rightarrow \pi^*$ transition, electron donating substituents generally cause a hypsochromic shift of these bands [22]. An example of this shift is seen when Ganesh D. Sharma *et al.* [23] synthesized an (organic) cyanuric-based dye, and reported the UV–vis absorption spectra of the dye in THF displays absorption bands in the 400–450 nm region and two weaker Q bands in the 520–650 nm region which is seen in figure 3.

The UV–vis absorption spectrum of the dye adsorbed onto TiO_2 film (red color line) exhibits similar absorption characteristics with those in solution, but these are broader (figure 3.). This is credited to the anchoring of the dye through its carboxylic acid

groups to TiO_2, a portent that is frequently observed in the spectral responses of organic sensitizers with carboxylic acid groups adsorbed onto TiO_2 films [23]. The width of the UV–vis absorption spectrum of the dye adsorbed onto TiO_2 designates its efficient light harvesting capability, thus making it suitable for usage as sensitizer in DSSCs.

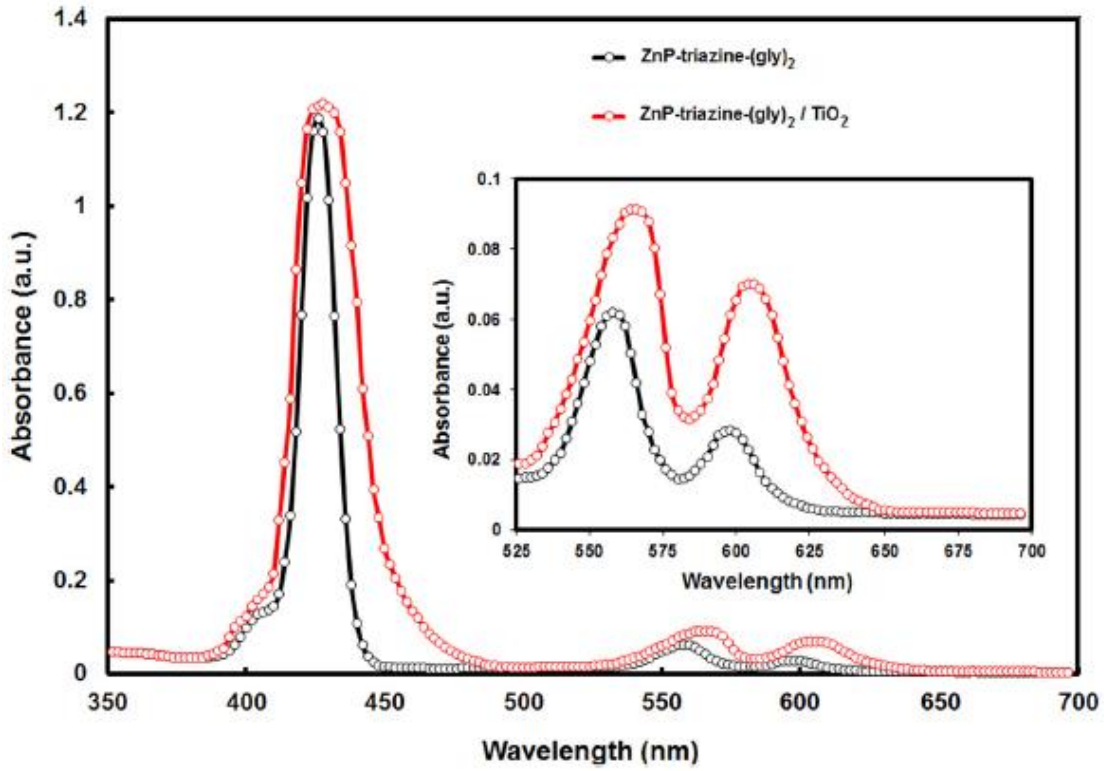

Figure 3. UV–vis absorption spectra of a cyanuric-based dye (ZnP-triazine-$(gly)_2$) in THF solution (black color) and ZnP-triazine-$(gly)_2$ adsorbed onto TiO_2 film (red color) [23].

3. RESEARCH METHODS

3.1 Research Design

The research will be both quantitative and qualitative. The quantitative part will involve determining at what wavelength the DSSCs exhibit bands using Ultraviolet-Visible Spectroscopy, whereas the qualitative part will involve determining the functional groups present in the DSSCs using Infrared Spectroscopy and investigating their chemosensing properties by monitoring colour changes of the DSSCs in response to certain stimuli.

3.2 Procedure

3.2.1 Synthesizing the dyes

The diagrams below show the fragments of the target dyes to be synthesized;

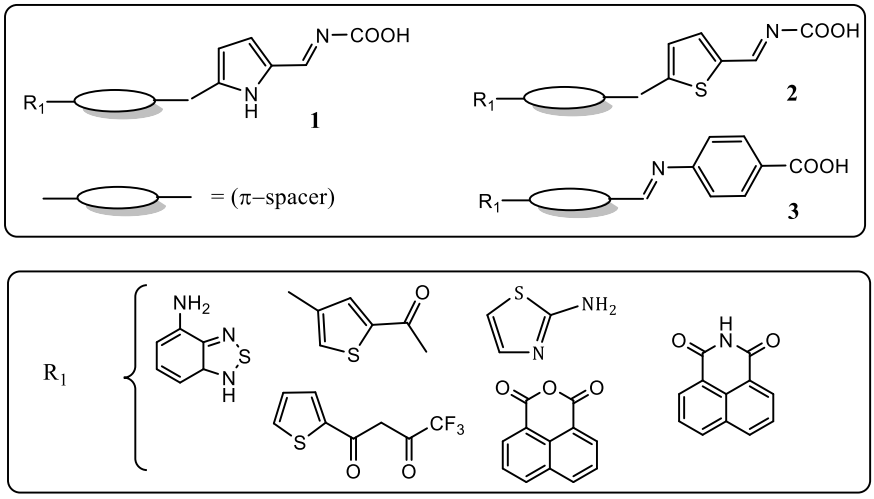

Where R_1 = π-electron systems from thiophene-based groups which absorb light in the visible region.

Figure 4. Molecular structure of the target dyes

3.2.2 Investigating the effect of solvatochromism

The polarity of the solvent affects the absorption of light by the dyes. Solvatochromatic effects will be investigated in to help determine which solvent is best to be used during the research study. This will be done by mixing the solvent and the dyes to see which solvent produces broader/sharper peaks using UV-Vis Spectroscopy.

3.2.3 Characterizing the organic-based DSSCs using spectroscopic techniques

UV-Vis spectroscopy, Proton Nuclear Magnetic Resonance (^{1}H NMR), Infrared, Elemental analyser and Fluoroscence spectroscopy will all be used to characterize the dyes.

3.2.4 Investigating their photo-response in the visible region

UV-Vis Spectroscopy will be used to determine the absorption bands of the dyes, and determine in which wavelength the bands occur.

3.2.5 Investigating the chemosensing properties

The dyes will be tested against certain ions in order to investigate their chemosensing properties. Colour change will indicate that the dyes are reacting with the ions.

3.3 Data Analysis

After the synthesis of the dyes, they will be analysed using UV-Vis analysis (UV-Vis spectrum). The Beer-Lambert Law ($A = \varepsilon bc$) will be used to determine the absorbance of the peaks that will be obtained from UV-Vis spectroscopy. From the equation, A

represents the absorbance, ε represents molar absorptivity, b is the path length of sample and c is the concentration of the sample. Infrared Spectroscopy will be used to determine the functional groups present in the structure while Fluorescence Spectroscopy will be used to investigate the emission properties.

4. EXPERIMENT

4.1 Materials and Instruments

Cyanuric chloride, 4-aminoacetophenone, hydrazine, naphtolbenzein, 2-aminothiozole, ethanol, acetonitrile. All reagents were of analytical grade and were used as received. Measurements were done at ambient temperature.

Absorption spectra were obtained on a PerkinElmer UV–Vis spectrometer (1 cm × 1 cm quartz cuvettes). Infrared data were obtained using TENSOR37 fourier-transform infrared spectrometer.

4.2 Synthesis of the dyes

The overall synthetic procedure is given in scheme 2. **Dye 1** was synthesized by cyanuric chloride and hydrazine refluxed for 5 hours in ethanol. The product (yellow crystals) was dried in a desiccator. After it was dried, the product together with naphtolbenzein were dissolved in ethanol and refluxed for 15 hours. This product (**Dye 1**) is yellow in colour and was filtered and continually washed with cold ethanol then dried in a desiccator for 48 hours. **Dye 2** was synthesized by cyanuric chloride and 4-aminoacetophenone refluxed for 5 hours in ethanol. The product (brown crystals) was dried in a desiccator. After it was dried, the product together with 2-aminothiozole were dissolved in ethanol and refluxed for 15 hours. This product (**Dye 2**) is brown in

colour and was filtered and continually washed with cold ethanol then dried in a desiccator for 48 hours.

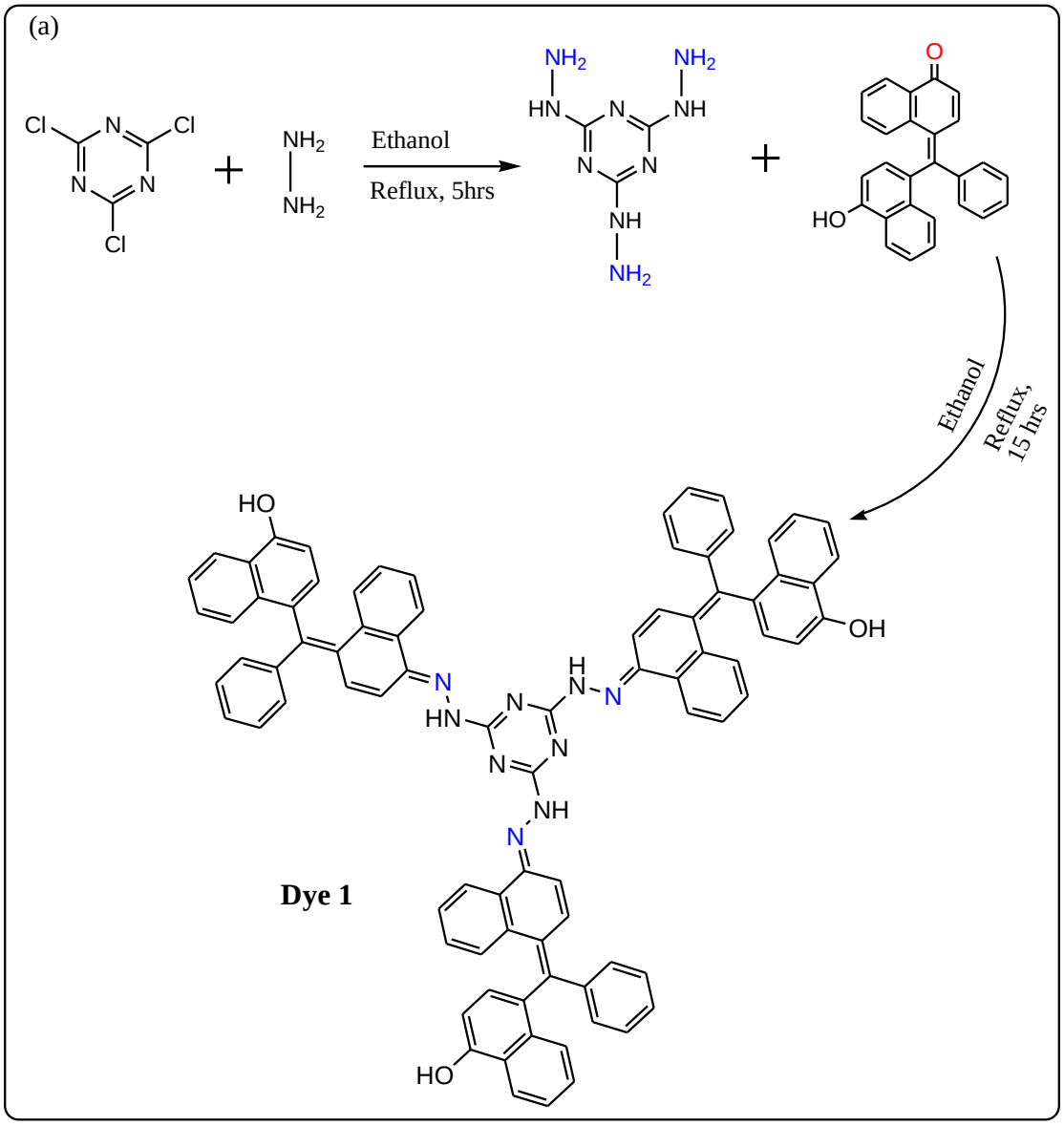

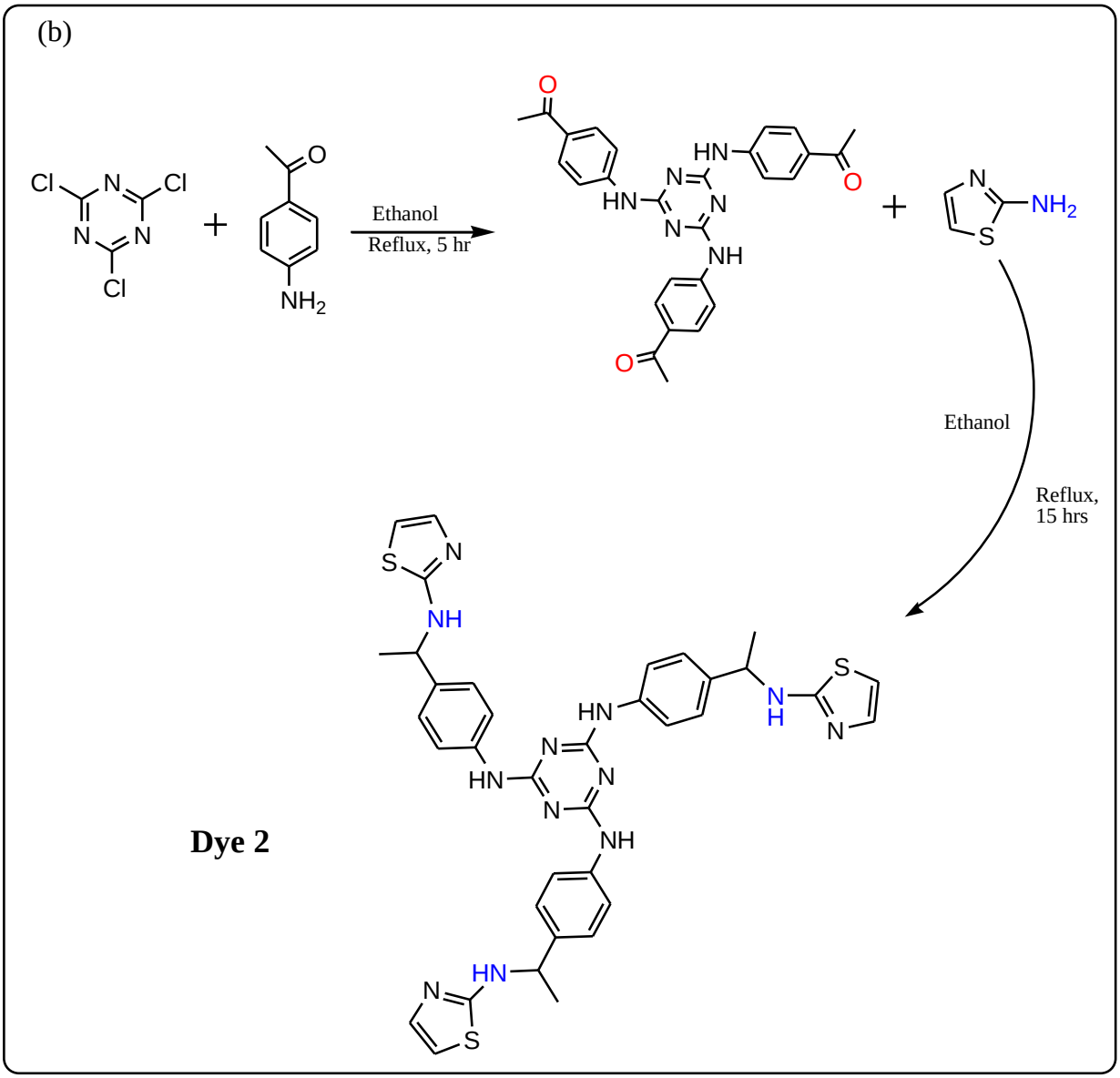

Scheme 2. Synthesis of (a) Dye 1 and (b) Dye 2.

5. RESULTS AND DISCUSSIONS

5.1. Photophysical property studies of the dyes

Figures 5 and 6 Elucidate the solution of the dyes (**Dye 1** & **Dye 2** respectively) in ethanol (1×10^{-5} mol.dm^{-3}) on the UV–Vis spectra. **Dye 1** gives rise to two absorption bands in the ultraviolet region at 330 nm and 380 nm, the bands are a result of π-π* transitions detected in π-conjugated systems (Cyanuric derivatives), there is also a band in the visible region at 420 nm which is assigned to an intramolecular charge transfer band from the donor nitrogen atoms [24]. **Dye 2** has overlapping bands at 450 nm and 470 nm (visible region) as seen in Figure 6, which are typically allocated to another localized excitation with a lower energy band produced by intramolecular charge transfer band from the donor nitrogen atoms.

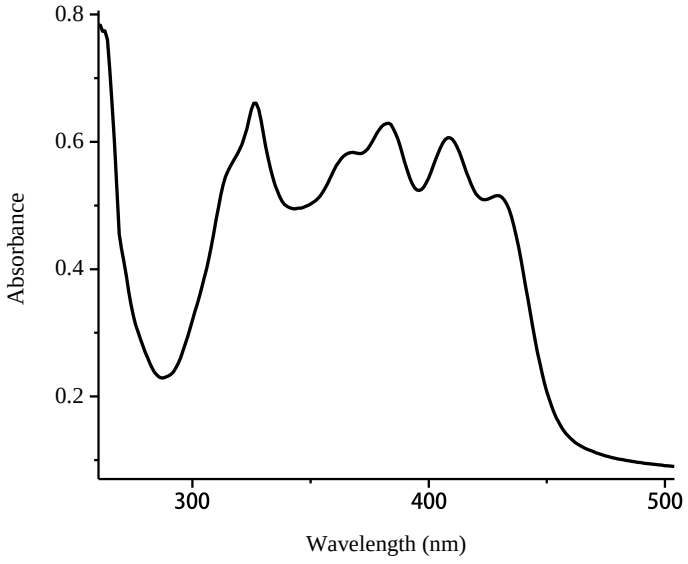

Figure 5. UV–Vis absorption spectra of Dye 1 in 1×10^{-5} mol·dm^{-3} Ethanol.

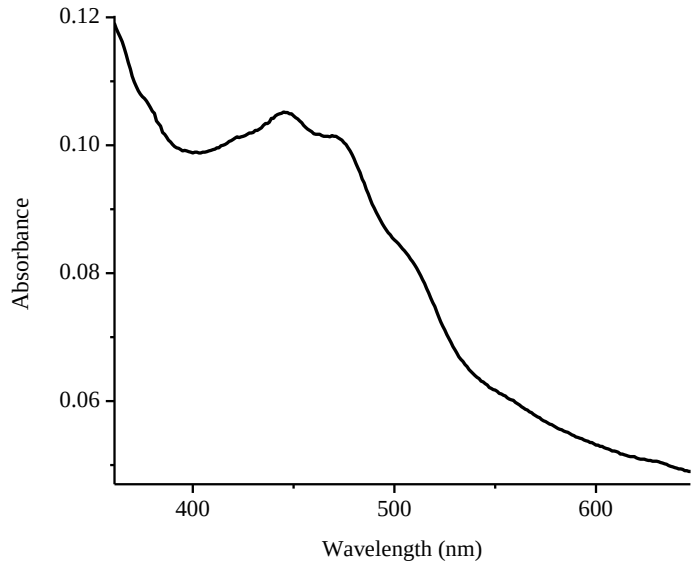

Figure 6. UV–Vis absorption spectra of Dye 2 in 1×10^{-5} mol·dm^{-3} Ethanol.

5.2 Solvatochromic studies of the dyes

The absorption characteristics of **Dye 1** and **Dye 2** were scrutinized and observed in a series of solvents with different polarities; acetonitrile, ethyl acetate, ethanol, methanol and toluene (1×10^{-5} mol.dm^{-3}) under UV–Vis light. **Dye 1** gives the highest molar extinction coefficients (hyperchromic effect) in ethanol, followed by acetonitrile, with the lowest (hypochromic effect) observed in methanol and ethyl acetate. **Dye 1** gives rise to bands in the following order; ethanol, acetonitrile, toluene, methanol and ethyl acetate with ethanol giving the highest bands and ethyl acetate giving the lowest bands (figure 7(a)), while **Dye 2** gives rise to bands in the following order; ethanol, acetonitrile, ethyl acetate, methanol and toluene, with ethanol giving the highest bands and toluene giving the lowest bands (figure 7(b)). **Dye 2** gives the highest molar extinction coefficients (hyperchromic effect) in ethanol, followed by acetonitrile, with the lowest (hypochromic effect) observed in methanol and Toluene.

(a)

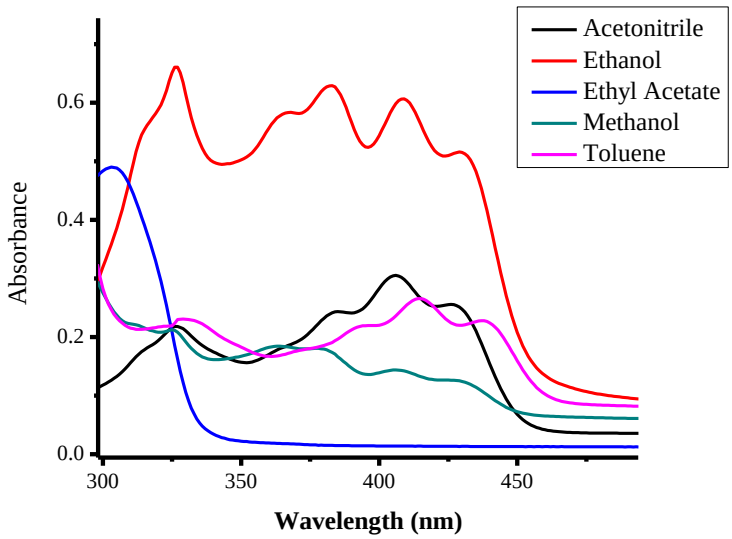

(b)

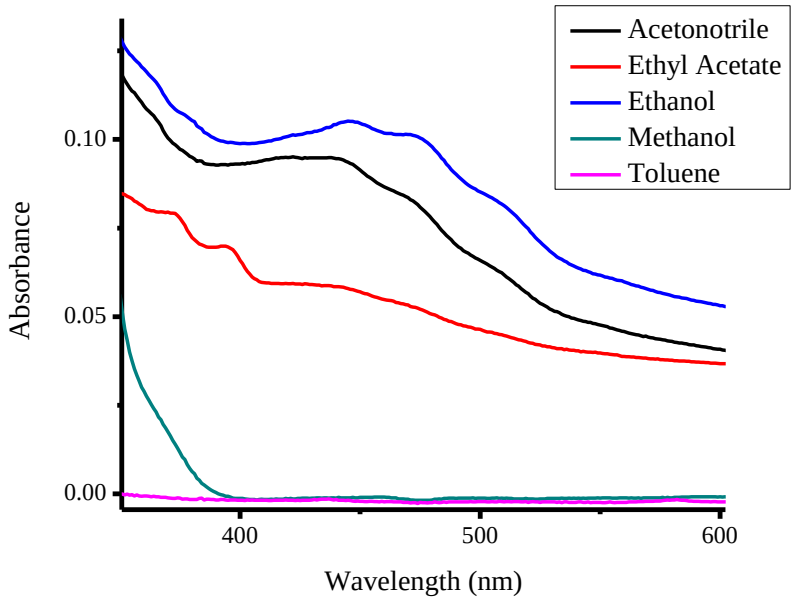

Figure 7. UV–Vis absorption spectra of (a) Dye 1 in 1×10^{-5}mol·dm^{-3} Acetonitrile, Ethyl Acetate, Ethanol, Methanol and Toluene; and (b) Dye 2 in 1×10^{-5}mol·dm^{-3} Acetonitrile, Ethyl Acetate, Ethanol, Methanol and Toluene.

In Tables 1 and 2, varying molar absorptivities of the dyes from different solvents are shown, with ethanol and acetonitrile showing highest extinction coefficients for both **Dye 1** and **Dye 2**, thus, having a prospective of being superior photon harvesters. Solvent polarities influence the photophysical properties of dye sensitizers. The absorption spectra and molar extinction coefficients contrast in locations and intensities respectively (Tables 1 and 2). Moreover, the dyes exhibited an extensive variety of feeble solubility in some of the solvents except acetonitrile and ethanol. Solvents such as toluene, ethyl acetate, methanol and tetrahydrofuran did not yield decent solubility for the dyes. As a result, ethanol was selected as a superior solvent because the dyes demonstrated a high grade of solubility at standard conditions.

Table 1: UV-visible absorption maxima of **Dye 1** in different solvents; (Acetonitrile, Ethyl Acetate, Ethanol, Methanol and Toluene)

Solvent	λ_{max} (nm)	ε ($L \cdot mol^{-1} \cdot cm^{-1}$)	λ_{onset} (nm)	E_{H-L} (eV) (band gap)
Acetonitrile	406	30000	484	2.56
Ethanol	326	63000	520	2.38
Methanol	383	19000	495	2.51
Ethyl acetate	303	2000	350	3.54
Toluene	415	27000	509	2.44

Table 2: UV-visible absorption maxima of **Dye 2** in different solvents; (Acetonitrile, Ethyl Acetate, Ethanol, Methanol and Toluene)

Solvent	λ_{max} (nm)	ε ($L \cdot mol^{-1} \cdot cm^{-1}$)	λ_{onset} (nm)	E_{H-L} (eV) (band gap)
Acetonitrile	441	9400	619	2.00
Ethanol	445	10000	632	1.96
Methanol	-	5000	-	-
Ethyl acetate	394	6900	610	2.03
Toluene	-	0	-	-

5.2.1 Solvatochromic effect on optoelectronic properties of the dyes

The optical and electronic characteristics of the dyes were examined and compared in diverse solvents with different polarities. In Tables 1 and 2, the dyes has exhibit fluctuating absorption varieties at different maxima, which interprets into different HOMO-LUMO gap values. The band gap is generally assessed as the energy gap of the HOMO-LUMO (organic compounds) or Valence-Conduction Bands (solid form dye systems). All the assessed band gaps of the dyes are within the visible region of the spectrum (except Dye 1 in ethyl acetate, 3.54 eV), indicating good potential as sensitizer for solar cells.

5.3 Infrared analysis of the dyes

The infrared spectra of the dyes is shown in figure 8. The spectra highlight features of cyanuric-based structures and the attached units (functional groups), as can be seen in Figure 8(a) the spectrum for **Dye 1** displaying a band at 1033.08 cm^{-1} which is assigned to the C-N stretch, primary amines, tertiary C, the band at 1325.8 cm^{-1} is assigned to C-N stretching (aromatic amine), the band at 1464.6 cm^{-1} is assigned to C-H stretching which is due to the methyl group, the band at 2981.3 cm^{-1} is due to C-H stretching (alkane), characteristic of aromatics, aliphatic and olefins in the lignin, the band at

3700.7 cm^{-1} is assigned to O-H stretching (alcohol). Figure 8(b) shows the bands for **Dye 2**. It is seen that **Dye 2** exhibited bands at 766.74 cm^{-1} which is assigned to C-H bending, typical for 1,2 disubstituted alkane group, it originates from a breathing mode of 1,3,5-triazine ring system [25], 1033.08 cm^{-1} which is assigned to the C-N stretch, primary amines, tertiary C, 2973.12 cm^{-1} due to C-H stretching (alkane), characteristic of aromatics, aliphatic and olefins in the lignin.

(a)

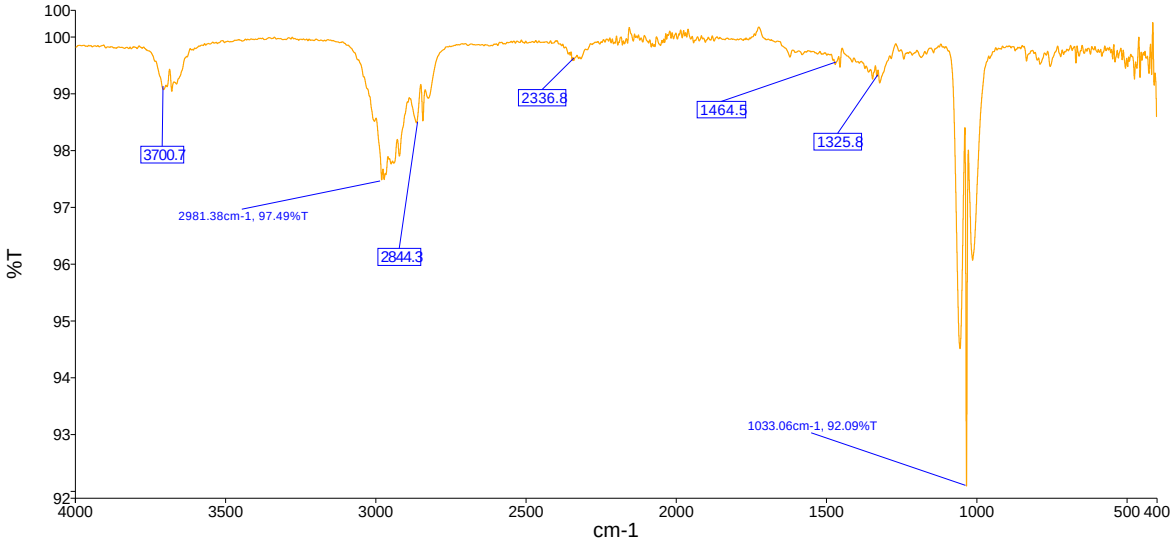

(b)

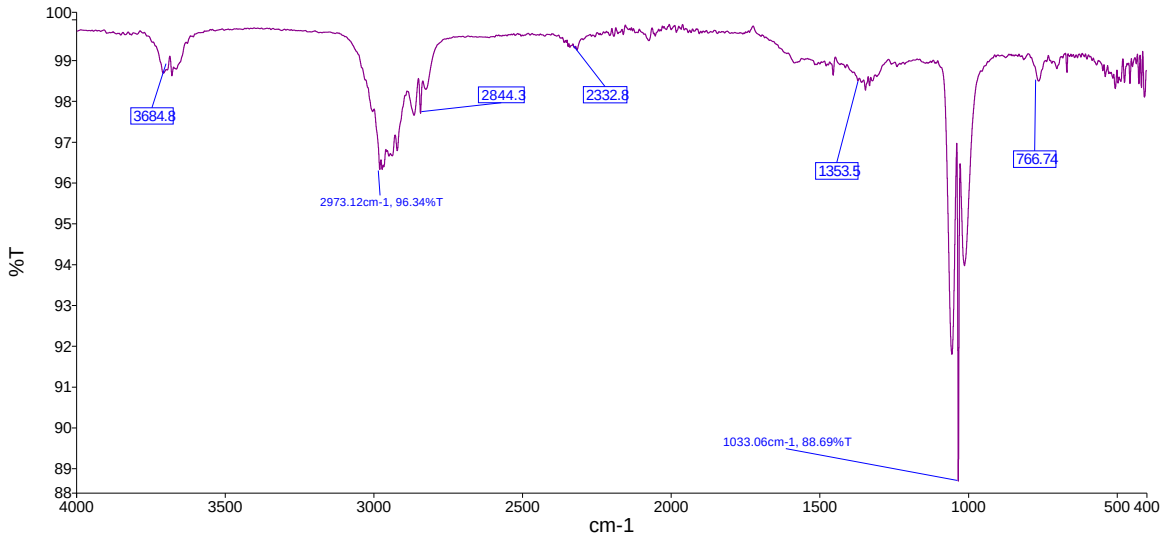

.

Figure 8. Infrared (IR) spectra of (a) Dye 1 and (b) Dye 2.

5.4 Naked eye detection test

5.4.1 Cation test

The cations Al^{+}, Co^{2+}, Cr^{2+}, Cu^{2+}, Fe^{2+}, K^{+}, Li^{+}, Pb^{2+} and Zn^{2+} were analyzed against The dyes (**Dye 1** and **Dye 2)** in ethanol (1×10^{-5} mol.dm^{-3}) to investigate their interactions respectively. With the naked eye test, it was seen that the presence of Cu^{2+} and Co^{2+} caused a colour change to **Dye 1** while for **Dye 2** Al^{+}, Cu^{2+}, Cr^{2+}, Fe^{2+} and Co^{2+} caused a colour change. On dropwise addition of Cu^{2+} to **Dye 1** the colour changed from orange to green, while the dropwise addition of Co^{2+} caused the dye to change from orange to dark orange as shown in Figure 9(a), which was detected by naked eyes. With regards to **Dye 2**, upon dropwise addition of Co^{2+} caused the colour to change from orange to red, the dropwise addition of Cu^{2+} to **Dye 2** caused the colour to change from orange to green while the dropwise addition of Fe^{2+} caused the colour to change from orange to light brown, Al^{+} caused the colour to change to orange and

finally Cr^{2+} changed the colour to light green as seen in figure 8(b). The rest of the cations did not produce a detectable change for both dyes; for **Dye 1**, Al^{+}, Cr^{2+}, Fe^{2+}, K^{+}, Li^{+}, Pb^{2+} and Zn^{2+} did not give rise to evident colour change, while for **Dye 2**, K^{+}, Li^{+}, Pb^{2+} and Zn^{2+} did not give rise to evident colour change, the colour lingered unchanged after their drop-wise additions to the dyes. Therefore, not all ions can interact with the dyes, only specific ions will give rise to a reaction.

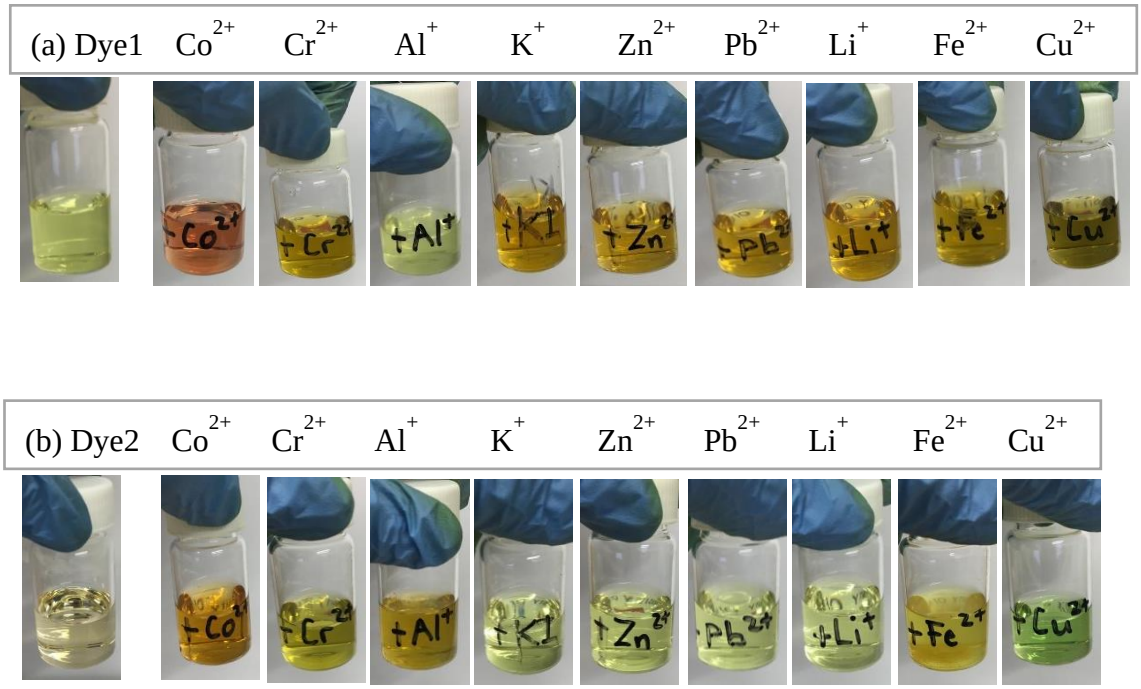

Figure 9. Showing color changes of (a) Dye 1 and (b) Dye 2 in ethanol at 1×10^{-5}M, after the additions of the cations respectively.

5.4.2 Anion test

The dyes were dissolved in ethanol (1×10^{-5} mol.dm^{-3}) and tested against the anions; SO_4^{2-}, Br^{-}, CN^{-}, F^{-}, NO^{-} and PO_4^{3-}. With the naked eye test, it was seen that the presence of SO_4^{2-}, CN^{-}, PO_4^{3-} and F^{-} caused a colour change to **Dye 1** while for **Dye 2** SO_4^{2-} and F^{-} caused a colour change. The dropwise addition of the anions to the dyes caused a slight colour change to both dyes as can be seen in figure 10. The dropwise addition

of SO_4^{2-} caused the colour of **Dye 1** to change from orange to pale blue, the dropwise addition of CN^- to **Dye 1** caused the colour to change to pale red, the dropwise addition of PO_4^{3-} to **Dye 1** caused the colour to change to pale red while the dropwise addition of F^- caused the colour to change to pale yellow as can be seen in figure 10(a). With regard to **Dye 2**, the dropwise addition of SO_4^{2-} to **Dye 2** caused the colour of the dye to change from light brown to pale brown while the dropwise addition of F^- to the dye caused to colour to change to pale grey, almost colourless as can be seen in figure 10(b). The rest of the anions did not produce a detectable change for both dye1 and **Dye 2**. With the anions, the colour changes are observed to be slight.

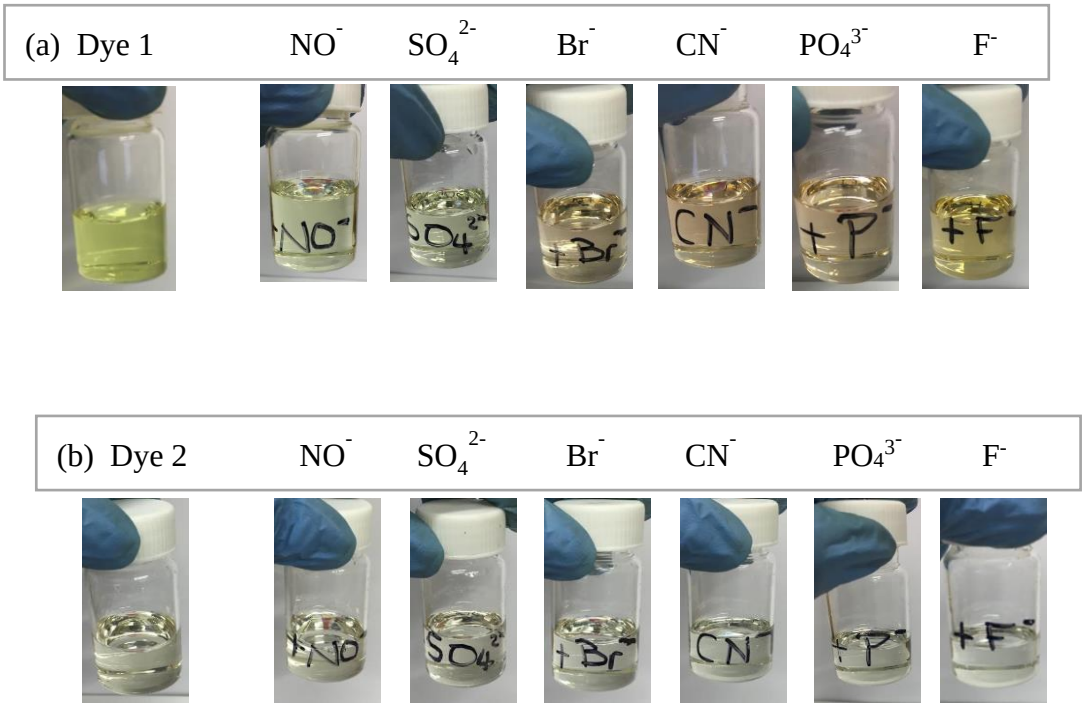

Figure 10. Showing color changes of (a) Dye 1 and (b) Dye 2 in ethanol at 1 × 10^{-5}M, after the additions of the anions respectively.

5.5 UV–Vis binding interaction studies

5.5.1 UV-Vis for cation studies

The UV-Vis analysis of **Dye 1** shows a spectra of the dye having two joint preliminary absorption bands at 420 and 350 nm increased gradually upon the molar addition of Al^{+} as shown in figure 11(a). On the other hand, the molar addition of Cu^{2+} to **Dye 1** showed a spectra with initial absorption bands at 420 and 340 nm decreasing each time the Cu^{2+} molar concentration is increased. Low energy absorption bands are seen at 500 and 300 nm as shown in Figure 11(b). The three isobestic points at 440, 330 and 270 nm show that a well-ordered interconversion between the complexed and uncomplexed species existed [24]. On the spectrum of **Dye 2** figure 12. The molar addition of Pb^{2+} to the dye gives an absorption band at 440 nm which is gradually decreasing as the molar concentration of Pb^{2+} is increased. It is interesting to note that it is indicated above that using the eye test, **Dye 2** changed colour when it was in contact with Al^{+}, Cu^{2+} and Co^{2+} indicating that the dye was reacting with these ions, however after UV-Vis analysis as before indicated, the three ions only Al^{+} was reacting with the dye while the other two were not reacting. The colour change is due to the fact that the two transition metal cations are coloured as such this affected the overall colour of the dye-ion mixture.

(a)

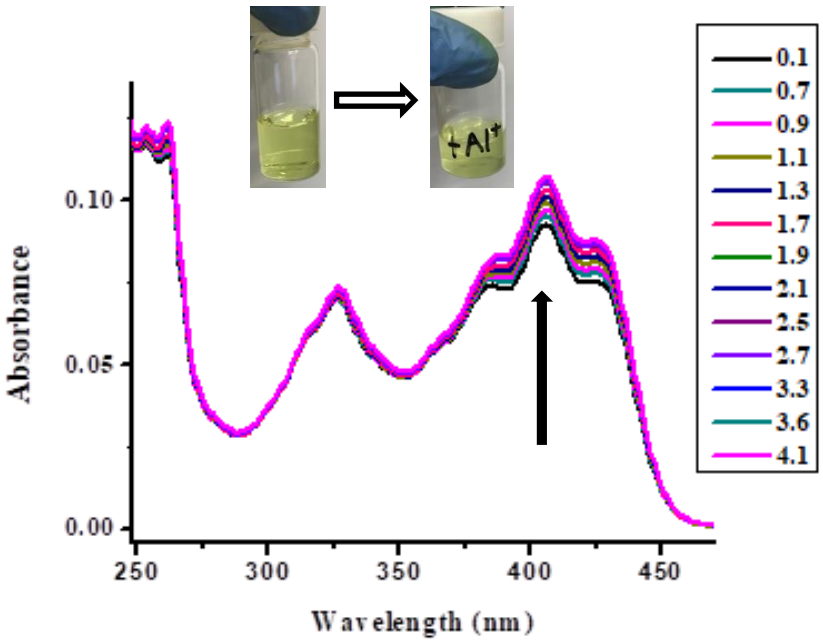

(b)

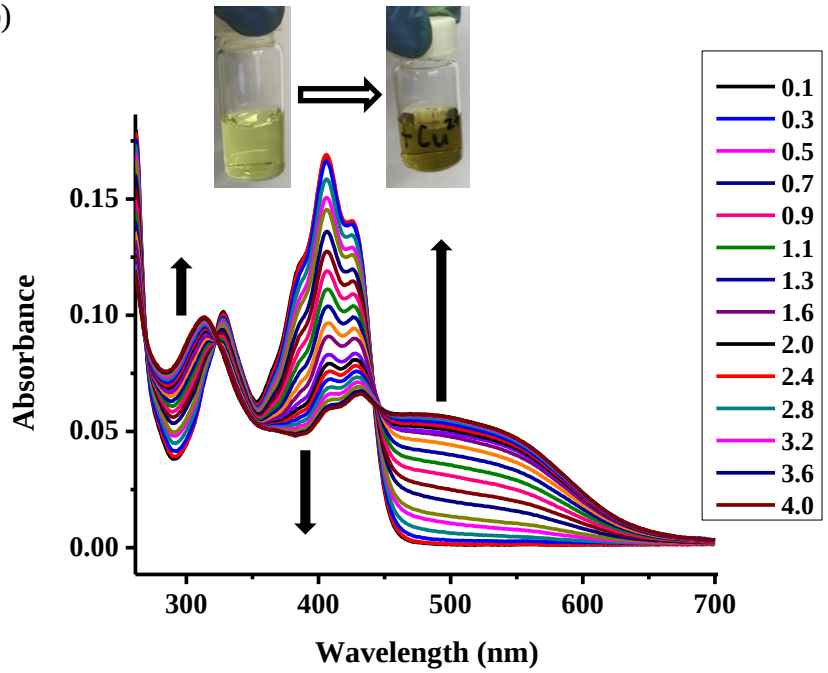

Figure 11. UV–Vis spectra of Dye1 in 1×10^{-5}mol·dm^{-3} ethanol after the addition of (a) Al^{+} and (b) Cu^{2+} cations.

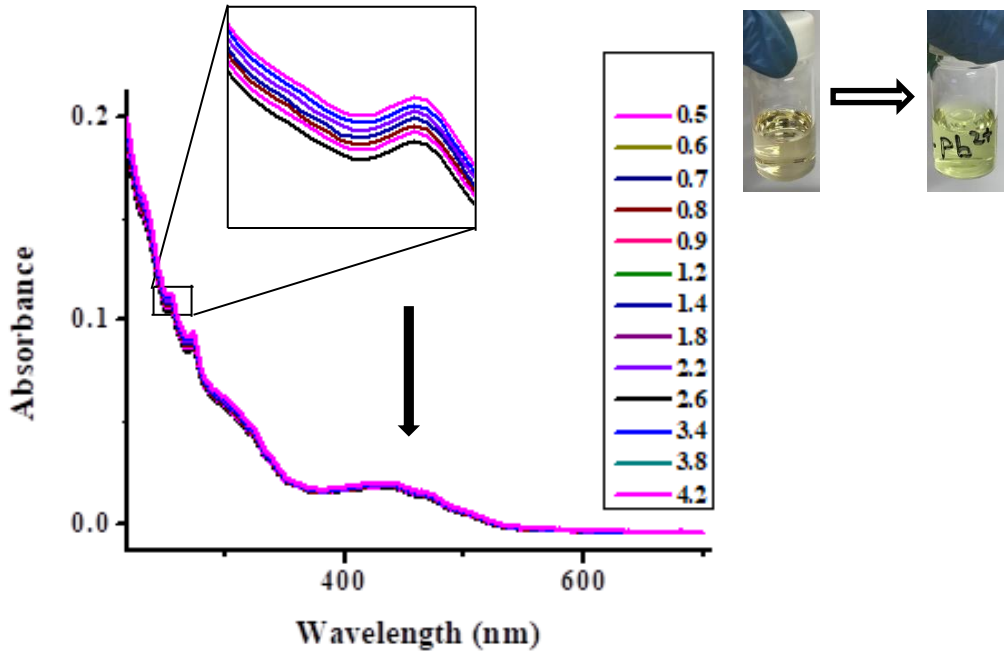

Figure 12. UV–Vis spectra of Dye 2 in 1 × 10^{-5}mol·dm^{-3} ethanol after the addition of Pb^{2+} cation.

5.5.2 UV-Vis for anion studies

The UV-Vis analysis of **Dye 1** shows a spectra of the dye having two joint preliminary absorption bands at 300, 400 and 520 nm. The band at 400 nm decreased gradually upon the molar addition of CN^-, while the bands at 300 and 520 nm increased, as shown in figure 13(a). The two isobestic points at 320 and 450 nm show that a well-ordered interconversion between the complexed and uncomplexed species existed [24]. Figure 13(b) elucidates how the molar addition of SO_4^{2-} to **Dye 1** yields a spectra with initial absorption bands at 330, 420 and 500 nm, the band at 420 nm was increasing, while the band at 500 nm was decreasing each time the molar concentration of SO_4^{2-} is

increased. A low energy absorption band is seen at 500 nm which is increasing upon the molar addition of F^- to **Dye 1**, concurrently the band at 420 nm is decreasing as seen in figure 13(c). Upon the molar addition of PO_4^{3-} to Dye 1, the band at 420 is decreasing while the bands at 320 and 500 nm are increasing as seen in figure 13(d). The UV-Vis analysis of **Dye 1** display that of the anions that were analysed (SO_4^{2-}, Br^-, CN^-, F^-, NO^- and PO_4^{3-}), only CN^-,SO_4^{2-}, F^- and PO_4^{3-} reacted with the dye, thus **dye 1** was able to sense them as a chemosensor. The interaction of the anions (CN^-, SO_4^{2-}, F^- and PO_4^{3-}) with **Dye 1** yielded isobestic points, showing that a well-ordered interconversion between the complexed and uncomplexed species existed. On the other hand, UV-Vis analysis of **Dye 2** with the anions (SO_4^{2-}, Br^-, CN^-, F^-, NO^- and PO_4^{3-}), displays that only SO_4^{2-} and F^- exhibited the occurrence of a reaction with **Dye 2**. The molar addition of SO_4^{2-} shows the bands at 330, 400 and 500 nm all increasing simultaneously as seen in figure 14(a). The molar addition of F^- to **Dye 2** gives a similar effect, the bands at 330 and 400 nm increase as the molar concentration of F^- increases as seen in figure 14(b).

(a)

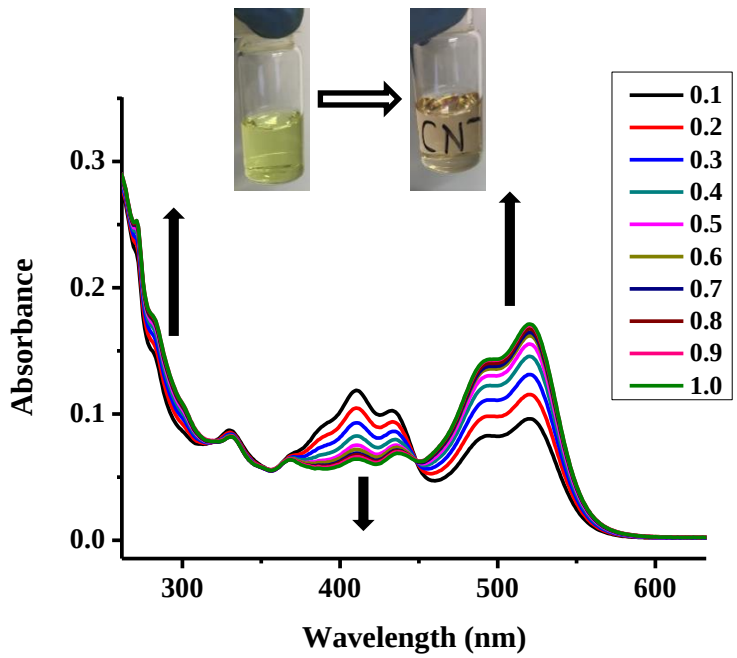
CN⁻
Absorbance
0.0
0.1
0.2
0.3
300
400
500
600
Wavelength (nm)
0.1
0.2
0.3
0.4
0.5
0.6
0.7
0.8
0.9
1.0

(b)

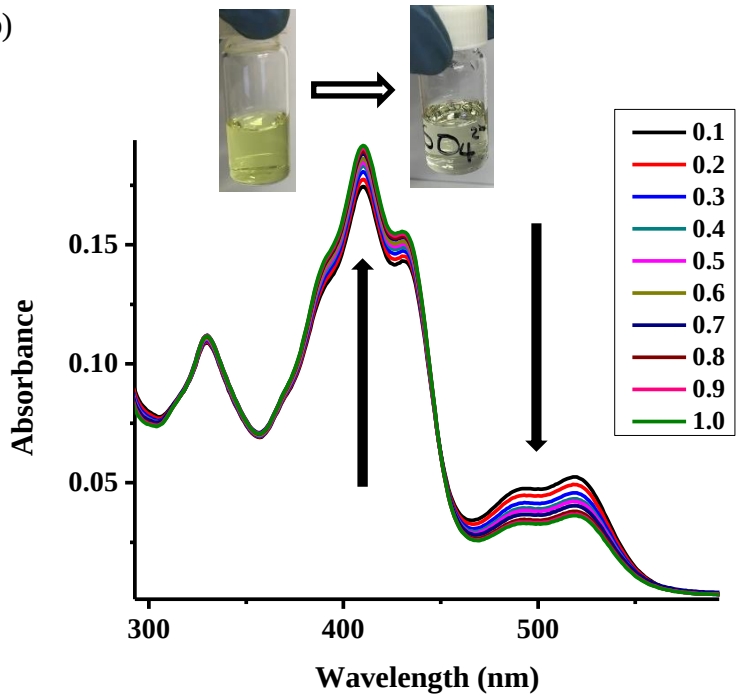
Absorbance
0.05
0.10
0.15
300
400
500
Wavelength (nm)
0.1
0.2
0.3
0.4
0.5
0.6
0.7
0.8
0.9
1.0

(c)

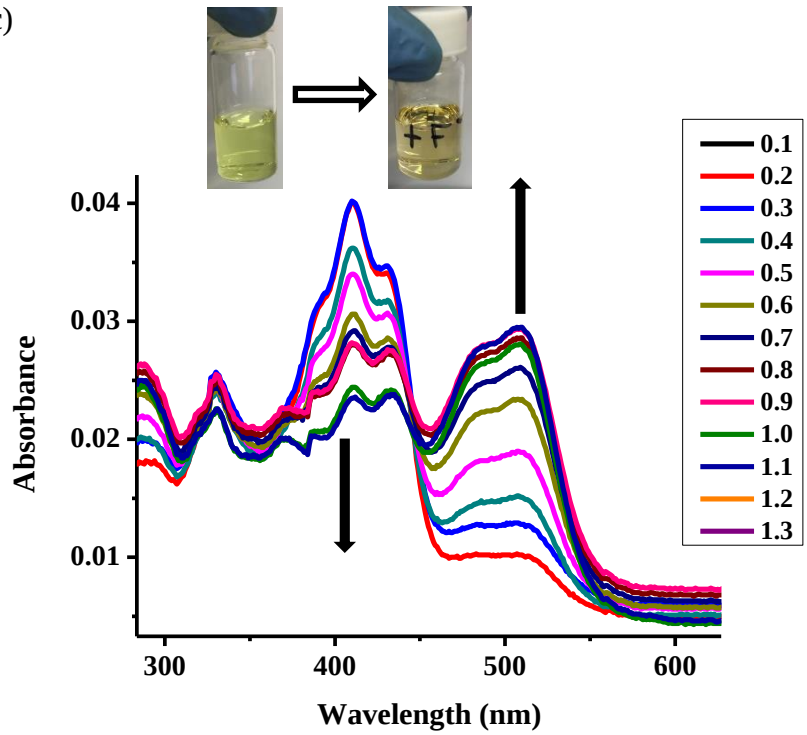

(d)

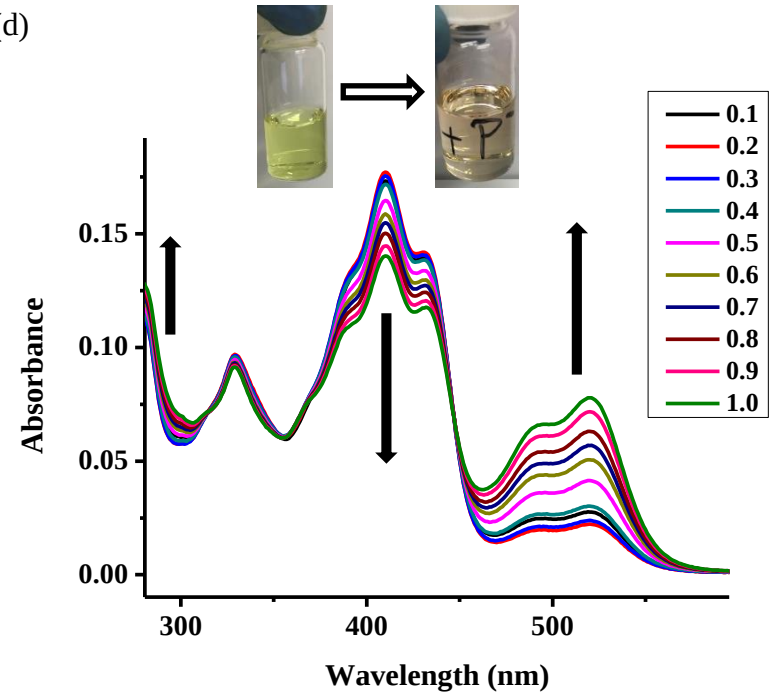

Figure 13. UV–Vis spectra of Dye 1 in 1 × 10^{-5}mol·dm^{-3} ethanol after the addition of (a) CN^-, (b) SO_4^{2-}, (c) F^- and (d) PO_4^{3-} anions.

(a)

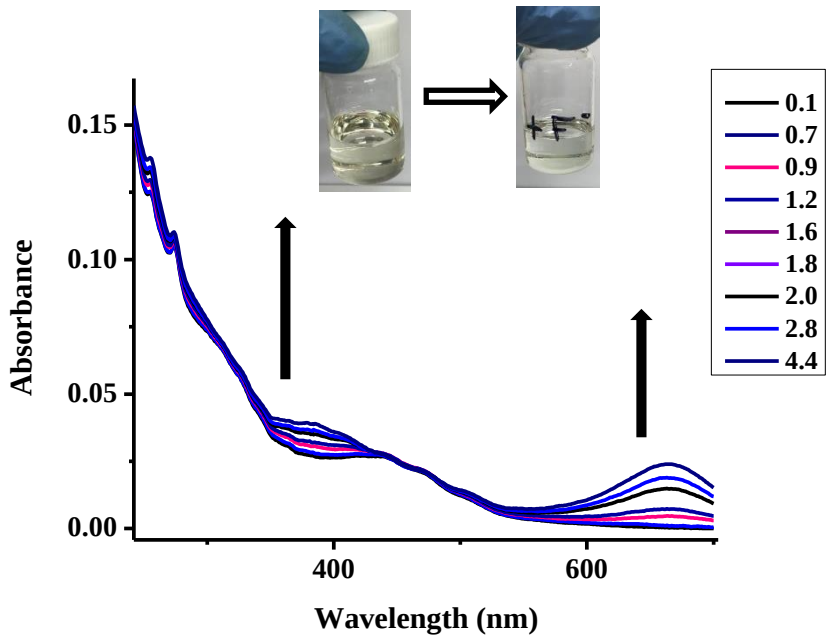

(b)

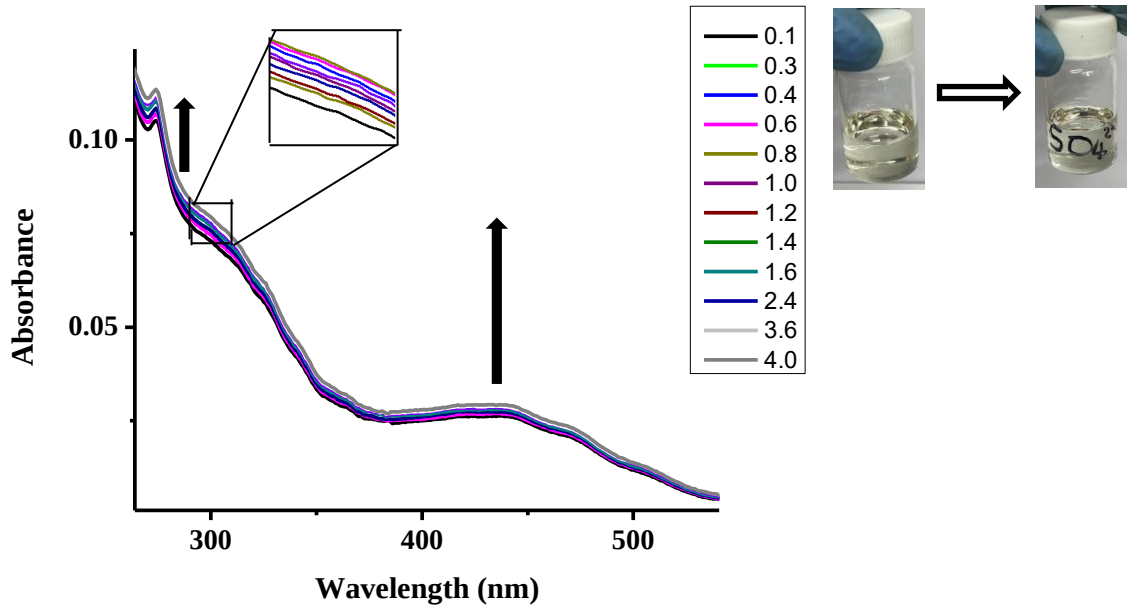

Figure 14. UV–Vis spectra of Dye 2 in 1 × 10^{-5}mol·dm^{-3} ethanol after the addition of (a) F^- and (b) SO_4^{2-} anions.

6. CONCLUSIONS

Two cyanuric-based dyes were synthesized (**Dye 1** and **Dye 2**) with different π-conjunction structures. **Dye 1** is covalently linked with hydrazine and benzoin while **Dye 2** is covalently linked with 4-aminoacetophenone and 2-aminothiozole. Both dyes give rise to absorption bands in the visible region and near infrared of the spectrum demonstrating prospect for utilization as dyes in dye sensitized solar cells. The observation of how the dyes reacted with certain ions through naked eye detection and more notably spectral shifts demonstrate the dyes moreover act as sensors. **Dye 1** has a selective recognition of Al^{+}, Cu^{2+}, SO_4^{2-}, CN^{-}, PO_4^{3-} and F^{-} whereas **Dye 2** has a selective recognition of Pb^{2+}, SO_4^{2-} and F^{-}. Thus the dyes are not just suitable to be used as sensitizers they can also be used as sensors.

7. RECOMENDATIONS

From the research, it is realized that the dyes act as decent sensitizers as well as sensors, consequently the dyes can be used to battle the universal energy needs and also assist in detecting harmful ions. Pb^{2+}, Cu^{2+}, F^{-}, P^{-} and CN^{-} in the environment can be harmful if not monitored. Cyanuric based dyes continue to show research potency, thus a lot still need to be studied about the porphyrins. The dyes can expectantly act as worthy additions in relations to influencing researches toward the advancement and excellence of relevant goals.

8 REFERENCES

[1] Hu Y, Robertson N. Atypical organic dyes used as sensitizers for efficient dye-sensitized solar cells. *Frontiers of Optoelectronics*. 2016 Mar 1;9(1):38-43.

[2] Fitra M, Daut I, Gomesh N, Irwanto M, Irwan YM. Dye solar cell using Syzigium Oleina organic dye. *Energy Procedia*. 2013 Jan 1;36:341-8.

[3] Yan R, Qian X, Jiang Y, He Y, Hang Y, Hou L. Ethynylene-linked planar rigid organic dyes based on indeno [1, 2-b] indole for efficient dye-sensitized solar cells. *Dyes and Pigments*. 2017 Jun 1;141:93-102.

[4] Sharma GD, Angaridis PA, Pipou S, Zervaki GE, Nikolaou V, Misra R, Coutsolelos AG. Efficient co-sensitization of dye-sensitized solar cells by novel porphyrin/triazine dye and tertiary aryl-amine organic dye. *Organic Electronics*. 2015 Oct 1;25:295-307.

[5] Bessho T, Zakeeruddin SM, Yeh CY, Diau EW, Grätzel M. Highly efficient mesoscopic dye-sensitized solar cells based on donor–acceptor-substituted porphyrins. *Angewandte Chemie International Edition*. 2010 Sep 3;49(37):6646-9.

[6] Bagher AM, Vahid MM, Mohsen M. Types of solar cells and application. *American Journal of optics and Photonics*. 2015 Aug 21;3(5):94-113.

[7] Yang YS, Do Kim H, Ryu JH, Kim KK, Park SS, Ahn KS, Kim JH. Effects of anchoring groups in multi-anchoring organic dyes with thiophene bridge for dye-sensitized solar cells. *Synthetic metals*. 2011 May 1;161(9-10):850-5.

[8] Bourass M, Amine A, Hamidi M, Bouachrine M. New organic dyes based on phenylenevinylene for solar cells: DFT and TD-DFT investigation. *Karbala International Journal of Modern Science*. 2017 Jun 1;3(2):75-82.

[9] He LJ, Wang J, Chen J, Jia R, Zhang HX. The effect of relative position of the π-spacer center between donor and acceptor on the overall performance of D-π-A dye: a theoretical study with organic dye. *Electrochimica Acta*. 2017 Jul 1;241:440-8.

[10] Fuse S, Yoshida H, Takahashi T. An iterative approach to the synthesis of thiophene-based organic dyes. *Tetrahedron Letters*. 2012 Jun 27;53(26):3288-91.

[11] Chaurasia S, Chen YC, Chou HH, Wen YS, Lin JT. Coplanar indenofluorene-based organic dyes for dye-sensitized solar cells. *Tetrahedron.* 2012 Sep 23;68(38):7755-62.

[12] Seo D, Park KW, Kim J, Hong J, Kwak K. DFT computational investigation of tuning the electron donating ability in metal-free organic dyes featuring a thienylethynyl spacer for dye sensitized solar cells. *Computational and Theoretical Chemistry*. 2016 Apr 1;1081:30-7.

[13] Zervaki GE, Angaridis PA, Koukaras EN, Sharma GD, Coutsolelos AG. Dye-sensitized solar cells based on triazine-linked porphyrin dyads containing one or two carboxylic acid anchoring groups. *Inorganic Chemistry Frontiers*. 2014;1(3):256-70.

[14] Biswas S, Pramanik A, Ahmed T, Sahoo SK, Sarkar P. Superiority of D–A–D over D–A type of organic dyes for the application in dye-sensitized solar cell. *Chemical Physics Letters*. 2016 Apr 1;649:23-8.

[15] Venkateswararao A, Thomas KJ, Lee CP, Ho KC. Synthesis and characterization of organic dyes containing 2, 7-disubstituted carbazole π-linker. *Tetrahedron Letters*. 2013 Jul 24;54(30):3985-9.

[16] Peng M, Dong B, Cai X, Wang W, Jiang X, Wang Y, Yang Y, Zou D. Organic dye-sensitized photovoltaic fibers. *Solar Energy*. 2017 Jul 1;150:161-5.

[17] Nachimuthu S, Lai KH, Taufany F, Jiang JC. Theoretical study on molecular design and optical properties of organic sensitizers. *Physical Chemistry Chemical Physics*. 2014;16(29):15389-99.

[18] Kuang D, Brillet J, Chen P, Takata M, Uchida S, Miura H, Sumioka K, Zakeeruddin SM, Grätzel M. Application of highly ordered TiO2 nanotube arrays in flexible dye-sensitized solar cells. *ACS nano*. 2008 Jun 24;2(6):1113-6.

[19] http://studentsrepo.um.edu.my/6535/5/CHAPTER_2_LITERATURE_REVIEW.pdf

[20] Kumar D, Wong KT. Organic dianchor dyes for dye-sensitized solar cells. *Materials Today Energy*. 2017 Sep 1;5:243-79.

[21] Lee CP, Li CT, Ho KC. Use of organic materials in dye-sensitized solar cells. *Materials Today*. 2017 Jun 1;20(5):267-83.

[22] Bohle M, Borzilleri RM, Döpp D, Döpp H, Herr RJ. Science of synthesis: Houben-Weyl methods of molecular transformations Vol. 17: Six-membered Hetarenes with two unlike or more than two heteroatoms and fully unsaturated larger-ring heterocycles.

[23] Sharma GD, Angaridis PA, Pipou S, Zervaki GE, Nikolaou V, Misra R, Coutsolelos AG. Efficient co-sensitization of dye-sensitized solar cells by novel porphyrin/triazine dye and tertiary aryl-amine organic dye. *Organic Electronics*. 2015 Oct 1;25:295-307.

[24] de la Hoz A, Sánchez-Migallón AM. Green synthesis of 1, 3, 5-triazines with applications in supramolecular and materials chemistry. *Targets Heterocycl. Syst*. 2016;20:139-73.

[25] Zhou C, Sun X, Yan J, Chen B, Li P, Wang H, Liu J, Dong X, Xi F. Thermo-driven catalytic degradation of organic dyes by graphitic carbon nitride with hydrogen peroxide. *Powder Technology*. 2017 Feb 15;308:114-22.

APPENDICES

The following UV-Vis spectra (titration) for **Dye 1** and **Dye 2** were not incorporated in the results segment as they did not display interaction between the dyes and the ions. No change to the spectra was observed as the concentration of the ions was increased, thus the dyes were not sensing these ions. **Dye 1** did not display interaction with Br^-, NO^-, Co^{2+}, Cr^{2+}, Fe^{2+}, K^+, Li^+, $Pb^{2+}$and Zn^{2+}while **Dye 2** did not display interaction with Br^-, CN^-, F^-, NO^-, PO_4^{3-}, Fe^{2+}, Al^+, Co^{2+}, Cr^{2+}, Cu^{2+}, L^+, Zn^{2+} and K^+, altogether the spectra can be comprehended in the figures below.

(a)

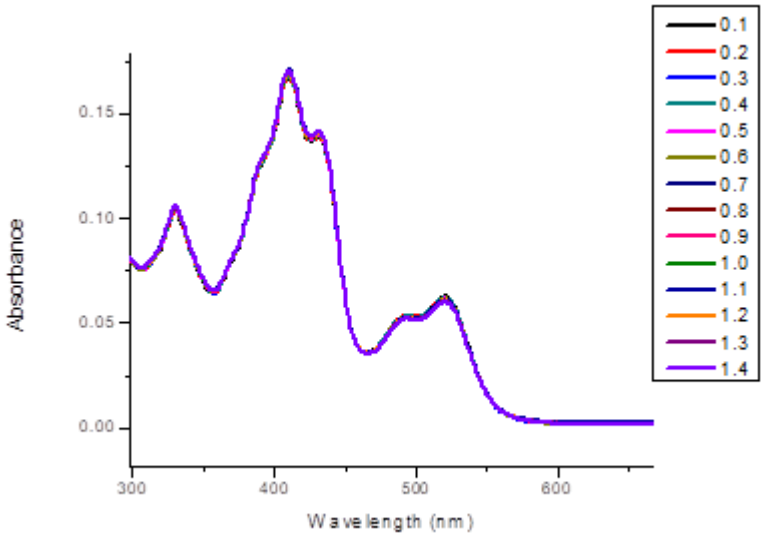

(b)

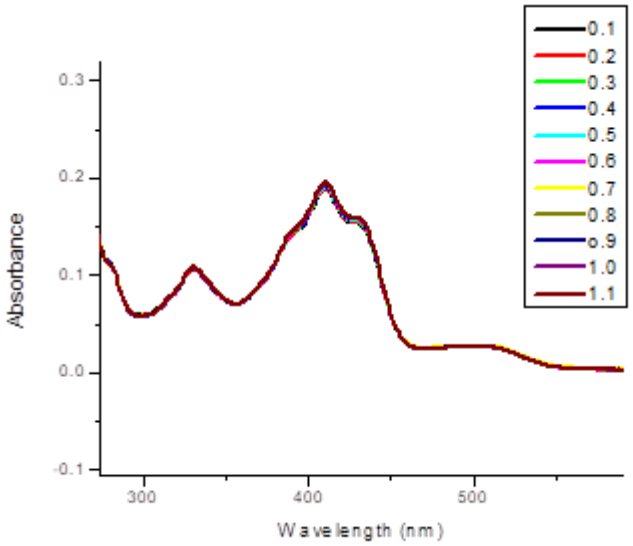
0.1
0.2
0.3
0.4
0.5
0.6
0.7
0.8
o.9
1.0
1.1
Absorbance
0.3
0.2
0.1
0.0
-0.1
300
400
500
Wavelength (nm)

(c)

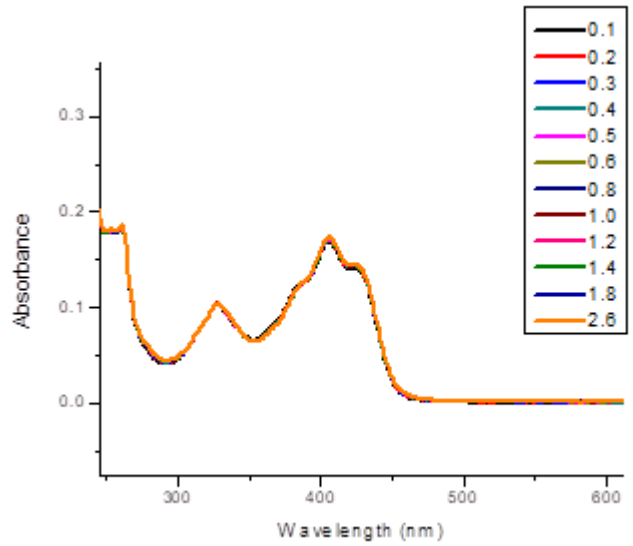
0.1
0.2
0.3
0.4
0.5
0.6
0.8
1.0
1.2
1.4
1.8
2.6
Absorbance
0.3
0.2
0.1
0.0
300
400
500
600
Wavelength (nm)

(d)

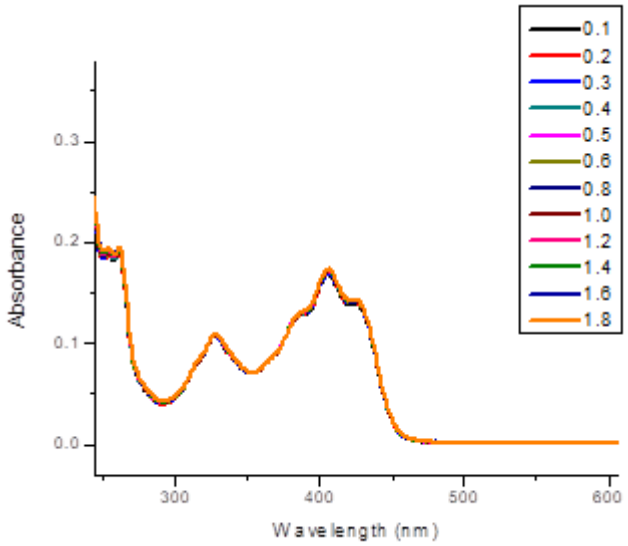
0.1
0.2
0.3
0.4
0.5
0.6
0.8
1.0
1.2
1.4
1.6
1.8
Absorbance
0.0
0.1
0.2
0.3
300
400
500
600
Wavelength (nm)

(e)

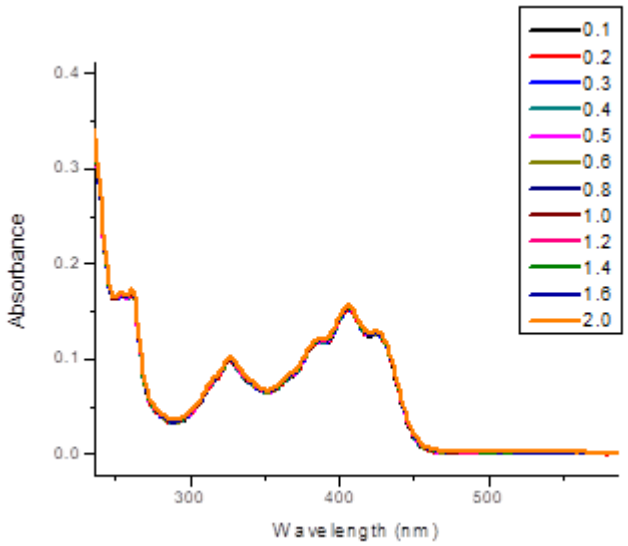
0.1
0.2
0.3
0.4
0.5
0.6
0.8
1.0
1.2
1.4
1.6
2.0
Absorbance
0.0
0.1
0.2
0.3
0.4
300
400
500
Wavelength (nm)

(f)

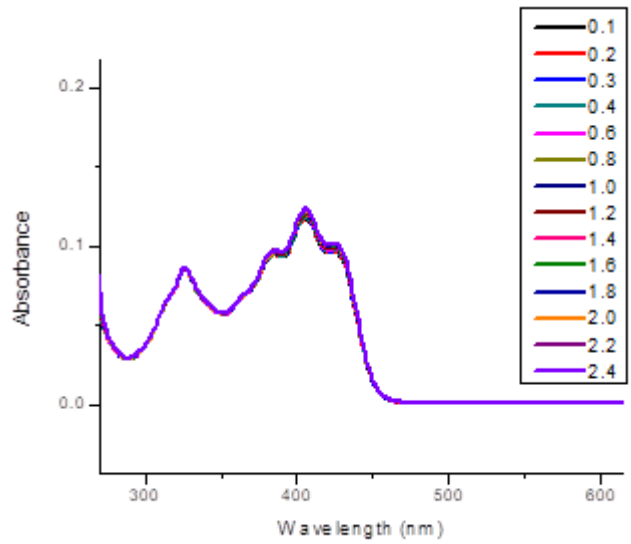
0.1
0.2
0.3
0.4
0.6
0.8
1.0
1.2
1.4
1.6
1.8
2.0
2.2
2.4
Absorbance
0.0
0.1
0.2
300
400
500
600
Wavelength (nm)

(g)

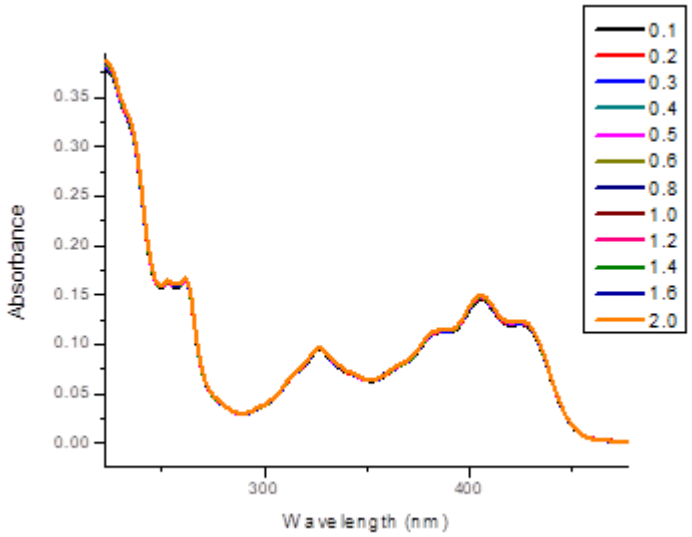
0.1
0.2
0.3
0.4
0.5
0.6
0.8
1.0
1.2
1.4
1.6
2.0
Absorbance
0.00
0.05
0.10
0.15
0.20
0.25
0.30
0.35
300
400
Wavelength (nm)

(h)

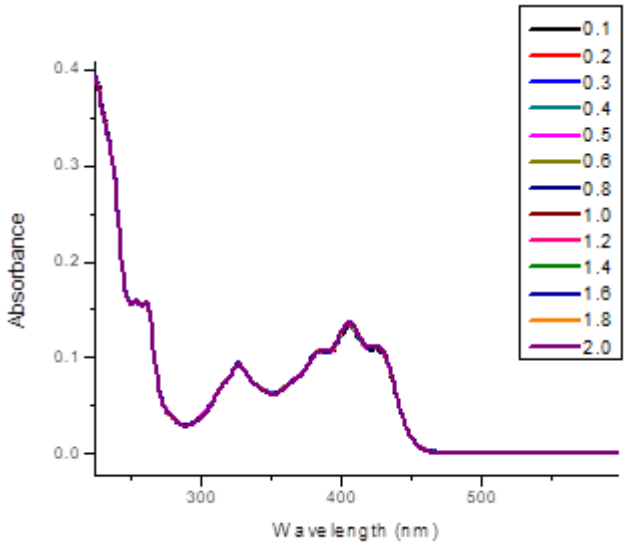

(i)

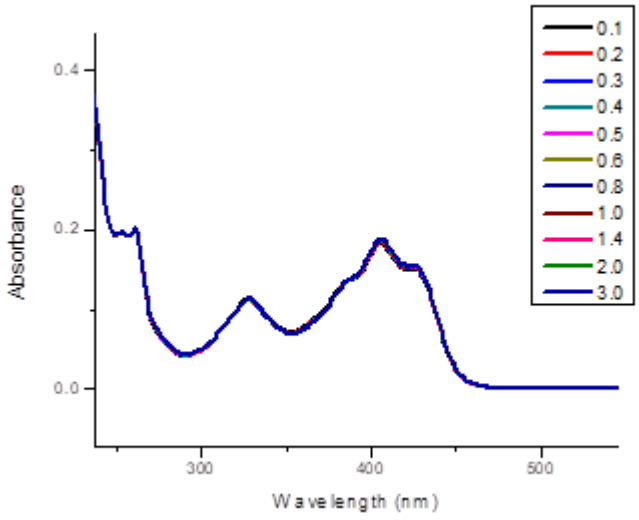

Figure 15. UV–Vis spectra of Dye 1 in 1 × 10^{-5}mol·dm^{-3} ethanol after the addition of (a) Br^-, (b) NO^-, (c) Co^{2+}, (d) Cr^{2+}, (e) Fe^{2+}, (f) K^+, (g) Li^+, (h) $Pb^{2+}$and (i) Zn^{2+}.

(a)

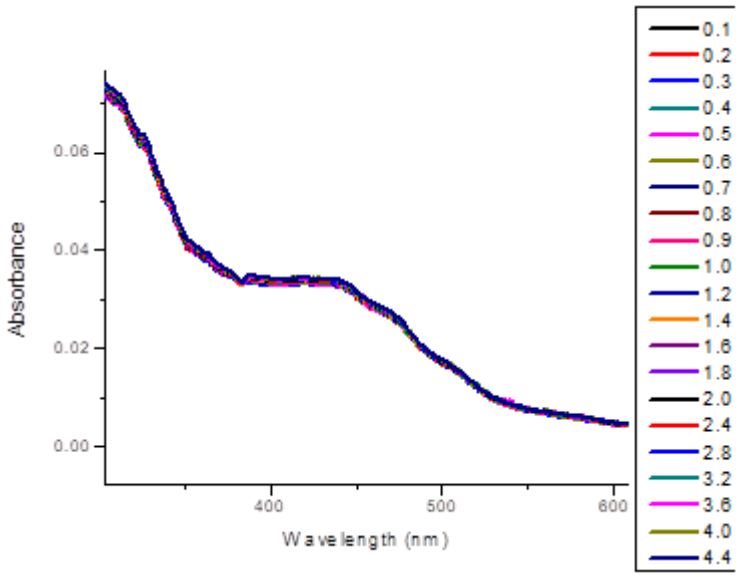
Absorbance
0.00
0.02
0.04
0.06
400
500
600
Wavelength (nm)
0.1
0.2
0.3
0.4
0.5
0.6
0.7
0.8
0.9
1.0
1.2
1.4
1.6
1.8
2.0
2.4
2.8
3.2
3.6
4.0
4.4

(b)

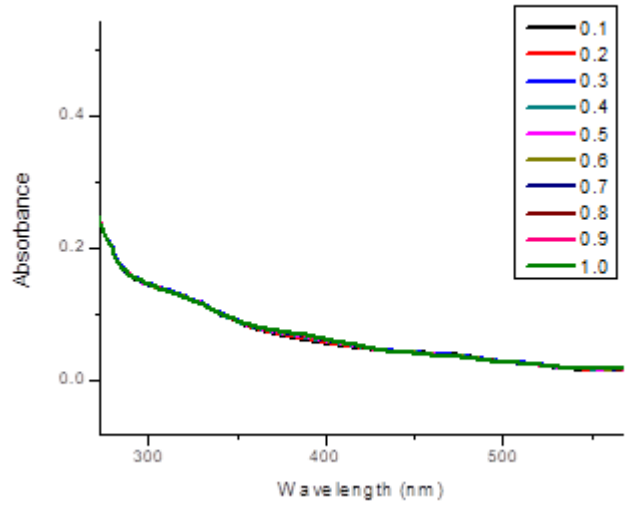
Absorbance
0.0
0.2
0.4
300
400
500
Wavelength (nm)
0.1
0.2
0.3
0.4
0.5
0.6
0.7
0.8
0.9
1.0

(c)

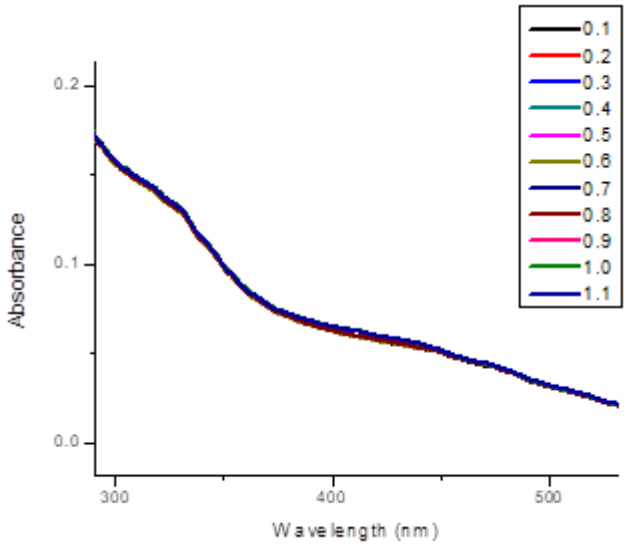
0.1
0.2
0.3
0.4
0.5
0.6
0.7
0.8
0.9
1.0
1.1
Absorbance
0.0
0.1
0.2
300
400
500
Wavelength (nm)

(d)

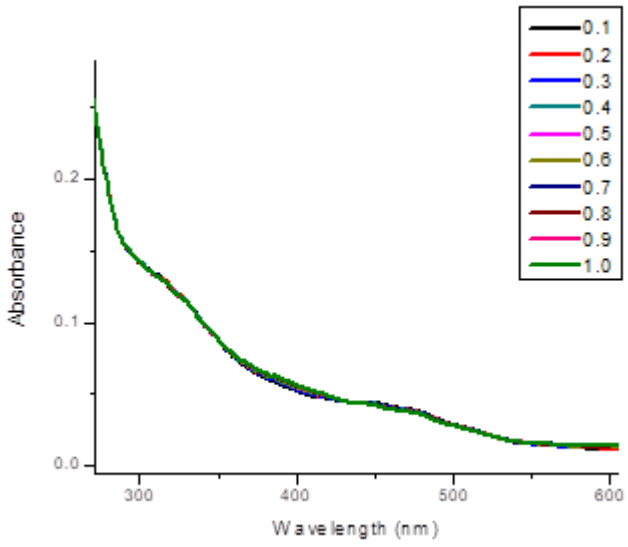
0.1
0.2
0.3
0.4
0.5
0.6
0.7
0.8
0.9
1.0
Absorbance
0.0
0.1
0.2
300
400
500
600
Wavelength (nm)

(e)

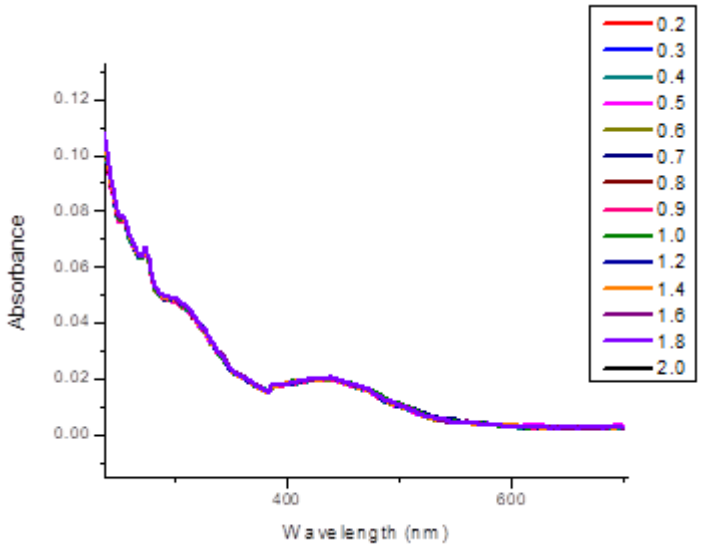
Absorbance
0.12
0.10
0.08
0.06
0.04
0.02
0.00
400
600
Wavelength (nm)
0.2
0.3
0.4
0.5
0.6
0.7
0.8
0.9
1.0
1.2
1.4
1.6
1.8
2.0

(f)

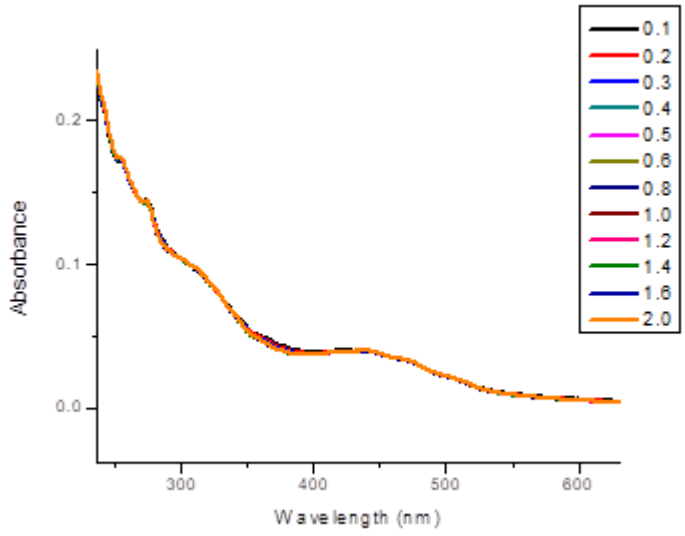
Absorbance
0.2
0.1
0.0
300
400
500
600
Wavelength (nm)
0.1
0.2
0.3
0.4
0.5
0.6
0.8
1.0
1.2
1.4
1.6
2.0

(g)

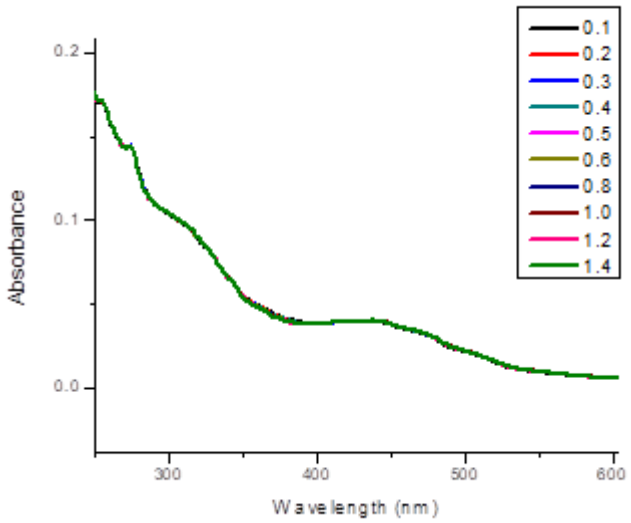
0.1
0.2
0.3
0.4
0.5
0.6
0.8
1.0
1.2
1.4
Absorbance
0.0
0.1
0.2
300
400
500
600
Wavelength (nm)

(h)

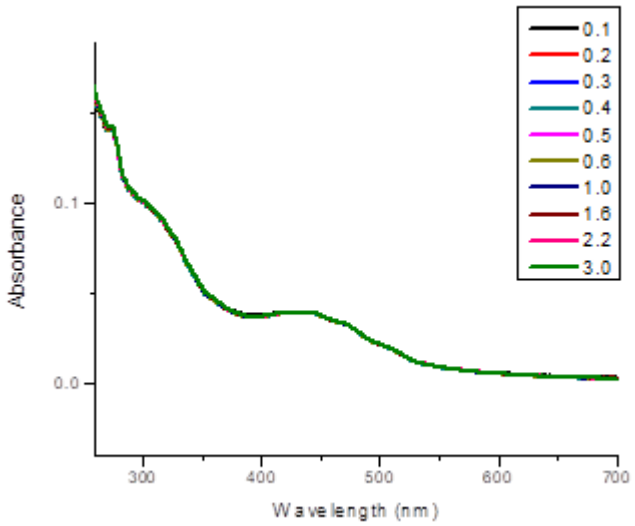
0.1
0.2
0.3
0.4
0.5
0.6
1.0
1.6
2.2
3.0
Absorbance
0.0
0.1
300
400
500
600
700
Wavelength (nm)

(i)

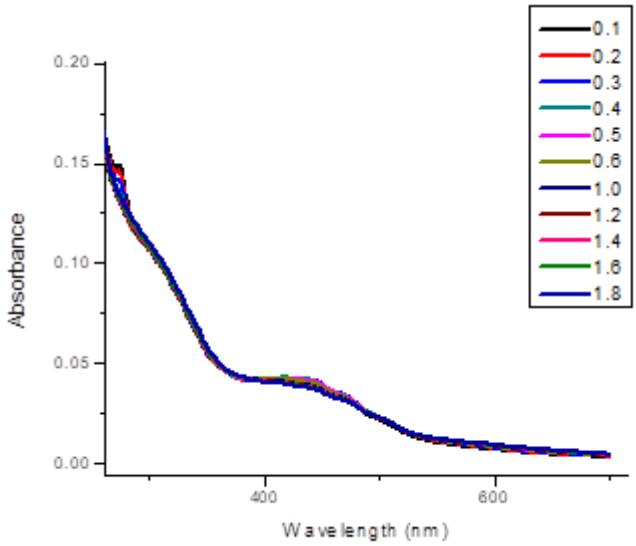
0.1
0.2
0.3
0.4
0.5
0.6
1.0
1.2
1.4
1.6
1.8
Absorbance
0.20
0.15
0.10
0.05
0.00
400
600
Wavelength (nm)

(j)

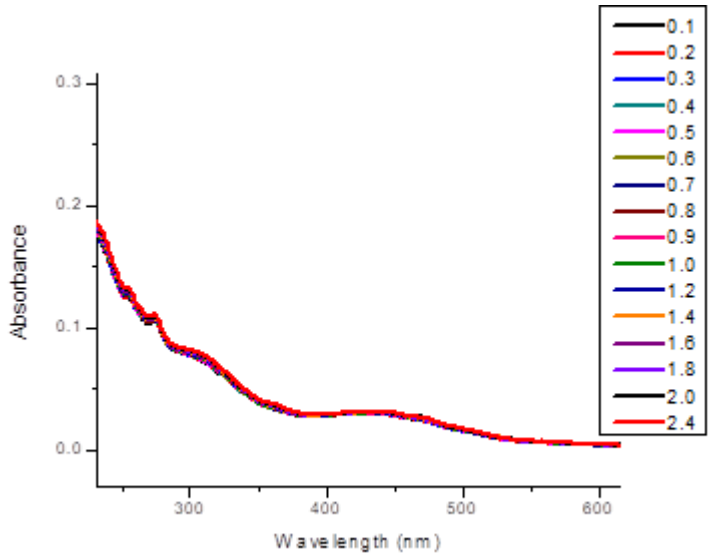
0.1
0.2
0.3
0.4
0.5
0.6
0.7
0.8
0.9
1.0
1.2
1.4
1.6
1.8
2.0
2.4
Absorbance
0.3
0.2
0.1
0.0
300
400
500
600
Wavelength (nm)

(k)

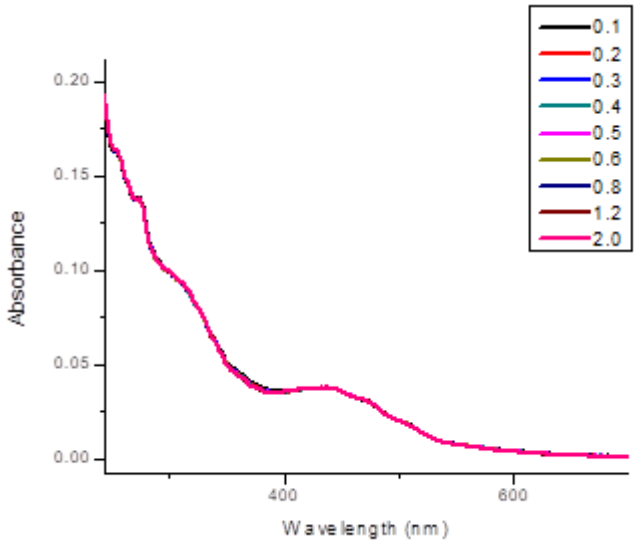

(l)

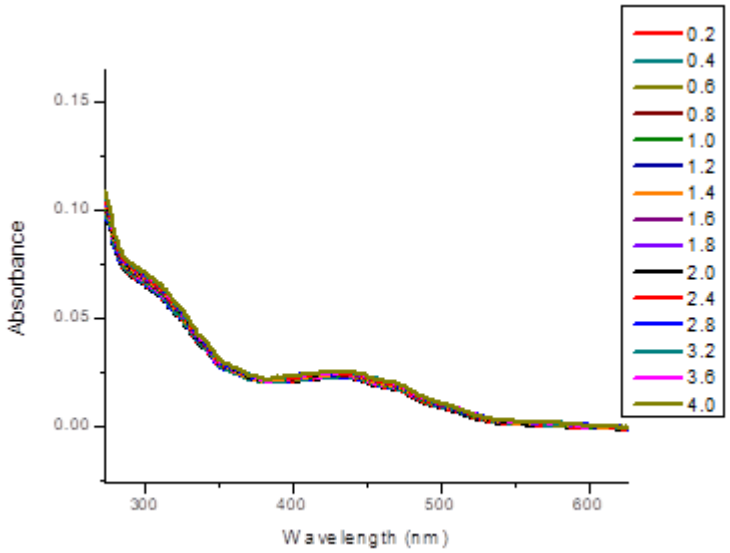

Figure 16. UV–Vis spectra of Dye 2 in 1×10^{-5}mol·dm^{-3} ethanol after the addition of (a) Br^-, (b) CN^-, (c) F^-, (d) NO^-, (e) PO_4^{3-}, (f) Fe^{2+}, (g) Al^+, (h) Co^{2+}, (i) Cr^{2+}, (j) Cu^{2+}, (k) L^+, (l) Zn^{2+}.

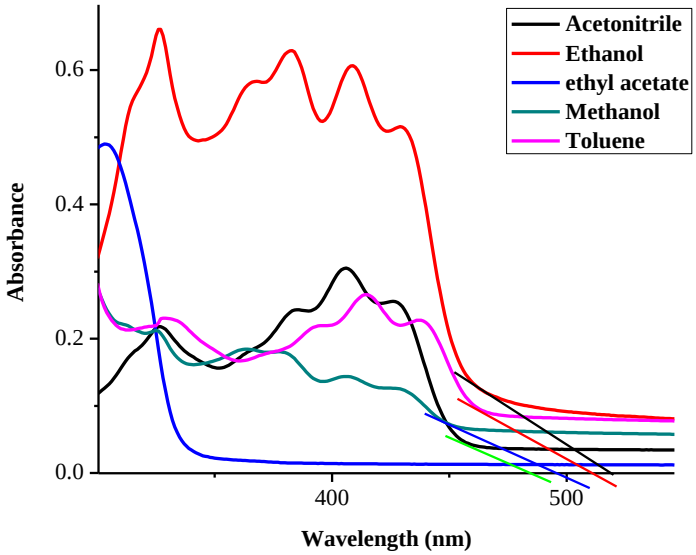

Figure 17. Absorption spectrum of Dye 1 in different solvents and optical onset band gap respectively.

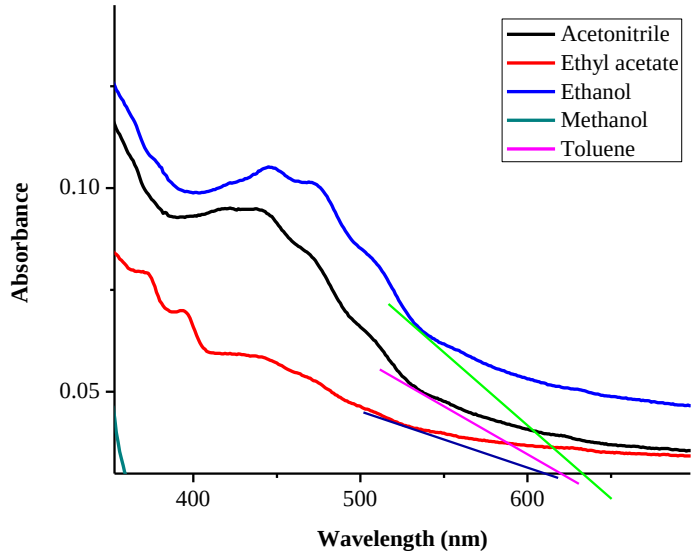

Figure 18. Absorption spectrum of Dye 2 in different solvents and optical onset band gap respectively.